Nuclear Safety
NEA/CSNI/R(2017)11
November 2017
www.oecd-nea.org

Benchmark Results on the Analytical Evaluation of the Fracture Mechanic Parameters K and J

Organisation de Coopération et de Développement Économiques
Organisation for Economic Co-operation and Development

English - Or. English

NUCLEAR ENERGY AGENCY
COMMITTEE ON THE SAFETY OF NUCLEAR INSTALLATIONS

NEA/CSNI/R(2017)11
Unclassified

Benchmark Results on the Analytical Evaluation of the Fracture Mechanic Parameters K and J

English - Or. English

ORGANISATION FOR ECONOMIC CO-OPERATION AND DEVELOPMENT

The OECD is a unique forum where the governments of 35 democracies work together to address the economic, social and environmental challenges of globalisation. The OECD is also at the forefront of efforts to understand and to help governments respond to new developments and concerns, such as corporate governance, the information economy and the challenges of an ageing population. The Organisation provides a setting where governments can compare policy experiences, seek answers to common problems, identify good practice and work to co-ordinate domestic and international policies.

The OECD member countries are: Australia, Austria, Belgium, Canada, Chile, the Czech Republic, Denmark, Estonia, Finland, France, Germany, Greece, Hungary, Iceland, Ireland, Israel, Italy, Japan, Korea, Latvia, Luxembourg, Mexico, Netherlands, New Zealand, Norway, Poland, Portugal, Slovak Republic, Slovenia, Spain, Sweden, Switzerland, Turkey, the United Kingdom and the United States. The European Commission takes part in the work of the OECD.

OECD Publishing disseminates widely the results of the Organisation's statistics gathering and research on economic, social and environmental issues, as well as the conventions, guidelines and standards agreed by its members.

NUCLEAR ENERGY AGENCY

The OECD Nuclear Energy Agency (NEA) was established on 1 February 1958. Current NEA membership consists of 33 countries: Argentina, Australia, Austria, Belgium, Canada, the Czech Republic, Denmark, Finland, France, Germany, Greece, Hungary, Iceland, Ireland, Italy, Japan, Korea, Luxembourg, Mexico, the Netherlands, Norway, Poland, Portugal, Romania, Russia, the Slovak Republic, Slovenia, Spain, Sweden, Switzerland, Turkey, the United Kingdom and the United States. The European Commission also takes part in the work of the Agency.

The mission of the NEA is:

– to assist its member countries in maintaining and further developing, through international co-operation, the scientific, technological and legal bases required for a safe, environmentally sound and economical use of nuclear energy for peaceful purposes;

– to provide authoritative assessments and to forge common understandings on key issues as input to government decisions on nuclear energy policy and to broader OECD analyses in areas such as energy and the sustainable development of low-carbon economies.

Specific areas of competence of the NEA include the safety and regulation of nuclear activities, radioactive waste management, radiological protection, nuclear science, economic and technical analyses of the nuclear fuel cycle, nuclear law and liability, and public information. The NEA Data Bank provides nuclear data and computer program services for participating countries.

COMMITTEE ON THE SAFETY OF NUCLEAR INSTALLATIONS

The Committee on the Safety of Nuclear Installations (CSNI) is responsible for NEA programmes and activities that support maintaining and advancing the scientific and technical knowledge base of the safety of nuclear installations.

The Committee constitutes a forum for the exchange of technical information and for collaboration between organisations, which can contribute, from their respective backgrounds in research, development and engineering, to its activities. It has regard to the exchange of information between member countries and safety R&D programmes of various sizes in order to keep all member countries involved in and abreast of developments in technical safety matters.

The Committee reviews the state of knowledge on important topics of nuclear safety science and techniques and of safety assessments, and ensures that operating experience is appropriately accounted for in its activities. It initiates and conducts programmes identified by these reviews and assessments in order to confirm safety, overcome discrepancies, develop improvements and reach consensus on technical issues of common interest. It promotes the co-ordination of work in different member countries that serve to maintain and enhance competence in nuclear safety matters, including the establishment of joint undertakings (e.g. joint research and data projects), and assists in the feedback of the results to participating organisations. The Committee ensures that valuable end-products of the technical reviews and analyses are provided to members in a timely manner, and made publicly available when appropriate, to support broader nuclear safety.

The Committee focuses primarily on the safety aspects of existing power reactors, other nuclear installations and new power reactors; it also considers the safety implications of scientific and technical developments of future reactor technologies and designs. Further, the scope for the Committee includes human and organisational research activities and technical developments that affect nuclear safety.

TABLE OF CONTENTS

EXECUTIVE SUMMARY

For most nuclear design and in-service inspection codes, fracture mechanics is used to evaluate the integrity of cracked components. The major parameters used in this kind of analysis are K and J which are used to estimate the crack-tip driving force. Different nuclear codes (e.g. RSE-M appendix 5 [1], AFCEN code: RCC-MRx appendix A16 [2], R6 rule [3], ASME B&PV Code Section XI [4], API 579 [5]) propose more or less sophisticated analytical solutions to estimate K and J. The solutions are based on compendia of stress intensity factors and limit loads that have been developed for common component geometries, type of defects and loading conditions. These codes also propose very different methods to incorporate the effects of thermal loads on K and J and to analyse cracks in a weld joint.

With respect to the various existing K and J procedures used in common nuclear design and in-service inspection codes, an activity titled “Benchmark on the analytical evaluation of the fracture mechanic parameters K and J for different components and loads”, was conducted within the subgroup of metallic components and structures of the Nuclear Energy Agency (NEA) Working Group on Integrity and Ageing of Components and Structures (WGIAGE) of the Committee on the Safety of Nuclear Installations (CSNI). The CSNI Activity Proposal Sheet (CAPS) was approved by the CSNI in December 2010 and the project was initiated during 2011. The principal objectives of the CAPS are to provide an overview and comparison of existing different nuclear code KJ estimation procedures through round robin analysis of several representative nuclear configurations. A secondary objective is to provide an opportunity for young engineers to learn about the various code methods and gain experience with their application.

The KJ benchmark activity was comprised of six analysis tasks. Each task represented a different nuclear component (e.g. pipes, elbows, welds) and/or set of conditions (e.g. mechanical loading, thermal loading, type and size of cracks). The tasks were ordered so that task 1 was the easiest task and addressed basic pressure and bending mechanical loads in simple geometries. The analysis complexity increased with each subsequent task to consider complex geometries and thermal and mechanical load combinations. Only K or J was estimated in any single task and the reference analysis for all tasks was a finite element analysis that was performed by the French Atomic Energy and Alternative Energy Commission (Commissariat à l'énergie atomique et aux énergies renouvelables, CEA). Specifically, task 1 addresses elastic stress intensity factor calculation (i.e. K_I), tasks 2 and 3 consider J calculation in cracked pipes, task 4 evaluates J estimation in cracked elbows, task 5 considers specific configurations (i.e. a pipe subject to an imposed displacement and a plate containing an embedded crack), and task 6 addresses J estimation in welds. A final task (7) consists of synthesising the results in order to identify, if possible, specific improvements for the different code procedures.

A total of 29 individuals representing 22 organisations participated in the benchmark activity, but not all of them provided solutions for all six analytical tasks. Most organisations provided solutions for the easiest task 1, but the number of participants decreased as the complexity of the task increased. For the most complex tasks, many participants only provided finite element solutions and not estimations using nuclear code procedures.

In general, it is noted that some of the estimates using code procedures are close to the baseline finite element results. However, other situations exist where the code estimates vary significantly from the finite element results. Also, in some cases, the estimates provided by different codes appear to differ significantly. While the reasons for these differences are not fully understood, it is expected that the following factors contribute to these differences.

1. The K and J evaluation procedures among the various codes that were considered in the benchmark are different and also have different intended conservative margins.
2. The K and J evaluation procedures may not always be clearly articulated and are therefore misapplied.

3. Some participants provided only one set of results while other participants revised their initial results.

4. Some participants were relatively inexperienced in applying the required code procedures.

5. In particular, factors 2 and 4 are synergistic in that misapplication of the required code procedures are more likely for inexperienced users, and misapplication also becomes more likely as the problem complexity increases.

The principal results and findings associated with each task are as follows:

- Task 1 – K_I: Several codes were used. The results are generally consistent and in good agreement with the finite element (FE) reference solutions. However, a few significant discrepancies exist, particularly among participants that applied the ASME code procedures. It is not clear if the discrepancies were the result of differences in models and their use or if they resulted from deficiencies or ambiguities within the ASME code itself.

- Tasks 2 and 3 – J in cracked pipes: Participants that used the AFCEN codes (a set of structural design and construction codes for pressurised water reactors published by French AFCEN association) generally provided homogeneous results that were in good agreement with the finite element solutions. Much more disparity exists among the results of participants that used the R6 code. Again, it is not clear if the discrepancies were the result of differences in models and their use, or if they resulted from deficiencies or ambiguities within the R6 code itself. Thermal loading can lead to large over-estimation of the J value, particularly for participants that used the BS and R6 codes.

- Task 4 – J in cracked elbows: Only the AFCEN code was used by participants for this task. Similar results were generally obtained among participants for simple mechanical loading with a few notable differences depending on how the bending moment was applied. Many of the participants also generally agreed with the finite element solutions when thermal loading was imposed, but a few results are significantly different.

- Task 5 – particular cases: only one analytical contribution, using the AFCEN code, was received for the pipe configuration with an imposed displacement. There is generally good agreement in the J estimation between the AFCEN code and the finite element solution. Also, for the plate configuration with an embedded crack, one participant only provided a finite element solution while the others all used the RCC-MRx code to estimate K_I. The participants that used the RCC-MRx code all obtained similar results but the code significantly overpredicts the reference finite element solution.

- Task 6 – J in weld: there were only a small number of participants for this task, and the task complexity seems to encourage contributors to perform finite element computations in parallel with estimations using code procedures. Both R6 and AFCEN procedures were used. The various finite element results exhibit differences which would require further investigation to understand. Also, the participants that used the R6 and AFCEN codes provided conservative results, although it should be noted that the R6 contributor considered residual stresses.

Based on the results of this analytical KJ benchmark round robin, some actions have already been taken to improve nuclear fracture mechanics codes. Between the years 2011 and 2016, some modifications and clarifications have been made to the description of code procedures in order to prevent misapplication of the code procedures. It is also clear that the procedures used among different codes can vary significantly and sufficient prescriptive guidance is not always provided within the codes. Both of these attributes cause increased complexity, which can lead to different results among users evaluating the same problem.

Therefore, it is recommended to use dedicated fracture mechanics software or tools that can help to guide the user through the application of the various code procedures. A discussion within WGIAGE has been started to consider additional investigations on specific KJ-analysis to check the efficiency of code modifications concerning root cause for discrepancies in comparable analysis results. It should be noted that the treatment of thermal loads and residual stresses differs significantly among the various codes. Future work is needed to develop appropriate methods for considering these effects and, ideally, harmonising their treatment within the various fracture mechanics codes.

LIST OF ABBREVIATIONS AND ACRONYMS

AFCEN	French association which publishes codes for design and construction for pressurised water reactors (Association française pour les règles de conception et de construction des matériels des chaudières électronucléaires)
AFCEN codes	A set of design and construction codes of AFCEN (e.g. RCC-C and RCC-MRx)
ASME	American Society of Mechanical Engineers
BARC	Bhabha Atomic Research Centre
BS	British Standard
CAPS	CSNI activity proposal sheet
CDSI	Circumferential internal semi-elliptical
CDAI	Circumferential internal axisymmetric
CEA	French Atomic Energy and Alternative Energy Commission (Commissariat à l'énergie atomique et aux énergies renouvelables)
C&S	Civil and structure
CEP	Combined Elastic-Plastic (optional estimation method J-integral under mechanical loading)
CLC	Corrected Limit Load (optional estimation method for mechanical loads)
CNRA	Committee on Nuclear Regulatory Activities
CRIEPI	Central Research Institute of Electric Power Industry
CSNI	Committee on the Safety of Nuclear Installations
CTR	Circumferential through wall defect
DFH	Ductile fracture handbook
EDF	Électricité de France
EFAM	Engineering flaw assessment method
EPRI	Electricity Power Research Institute (United States)

ETM	Engineering treatment method
F.E.	Finite element
FEM	Finite Element Methods
GDF-SUEZ/ENGIE	French multinational electric utility company
GRS	Gesellschaft für Anlagen- und Reaktorsicherheit
IAEA	International Atomic Energy Agency
IRSN	French Institute for Radiological Protection and Nuclear Safety (Institut de radioprotection et de sûreté nucléaire)
JRC	Joint Research Centre
JSME	Japan Society of Mechanical Engineers
KAERI	Korea Atomic Energy Research Institute
LTR	Longitudinal through wall defect
MJSAM	Fracture mechanical analysis tool developed by CEA (France)
NEA	Nuclear Energy Agency
LDSI	Longitudinal internal semi-elliptical
OECD	Organisation for Economic Co-operation and Development
PROST	Fracture mechanical analysis tool developed by GRS, Germany
RINPO	Research Institute of Nuclear Power Operation (China)
RS	Residual stress
SSM	Swedish Radiation Safety Authority
SINTAP	Structural integrity assessment procedures
WGIAGE	Working Group on Integrity and Ageing of Components and Structures (NEA)

1. INTRODUCTION

For many design and ageing considerations, fracture mechanics is needed to evaluate cracked components integrity. The major parameters used are the stress intensity factor K and the J-integral. Different codes (RSE-M appendix 5 [1], RCC-MRx appendix A16 [2], R6 rule [3], ASME B&PV Code Section XI [4], API 579 [5], …) propose more or less sophisticated analytical solutions to estimate these parameters. The solutions are based on compendia of stress intensity factors and limit loads for usual situations, in terms of component geometry, type of defect and loading conditions (e.g. EPRI Ductile Fracture Handbook [13], IWM formulation [14], SINTAP handbook [15], or ETM method [16]). In particular, these codes propose very different conservative methods to consider thermal loadings or cracks in a weld joint.

To achieve a comparative overview of the existing procedures, the benchmark BENCH-KJ has been proposed in the frame of the WGIAGE Group [6]. In this benchmark the different estimation schemes for representative industrial cases (pipes and elbows, mechanical or/and thermal loadings, different type and size of cracks) are compared with each other and to the reference analyses done by finite element method. On the one hand, the benchmark covers simple cases with basic mechanical loads like pressure and bending up to complex load combinations and complex geometries (cylinders and elbows) including cladding or welds. On the other hand, this benchmark proposed practical applications for young engineers, allowing them to get familiar with these analytical schemes.

The benchmark was separated into six tasks, with a progressive increase of difficulty from K_I evaluation to J estimation in welded joint.

This report gives an overview of the different benchmark tasks and presents the comparative assessment of the analysis results.

Note also that intermediate results were presented during the 2013 PVP conference [7] and other results during the 2015 SMiRT conference [10].

2. BENCHMARK OVERVIEW

2.1 Benchmark principles

Six tasks have been defined for the benchmark BENCH-KJ. The aim is to considered conventional situations in the first steps and then to go deeper into the difficulties by analysing more specific cases. A first set of cases has been defined by CEA to build the technical work, but all partners were invited to propose additional cases. It is not mandatory to contribute to all tasks. Each partner is free to propose only partial contributions (see Table 2.1-a). As the participation of the benchmark is based only on in-kind contributions, the content of each task has been defined to limit the effort of each partner.

Even if it focused on analytical procedures, partners were free to provide finite element (FE) results, which will be compared to the reference solution. The reference solutions used to define the original cases come from the FE data base developed jointly by AREVA, CEA and EDF for the development of the defect assessment procedures and related compendia of the RSE-M [1] and RCC-MRx codes [2]. 2D and 3D FE calculations have been performed on crack piping components (pipes and elbows). This data base includes more than 600 cases. Detail on the definition and the validation of this data base can be found in reference [8].

All application follows the rules of a blind test: the reference solution for a task is not communicated to the partners before the deadline fixed for the results submission. A participant number was attributed by CEA to each participant, which allowed results to be presented anonymously. A total of 22 companies were involved, participants are identified in Table 1.

Table 1: List of the benchmark participants

CEA	*France*	**IGCAR**	*India*	**Seoul University**	*Korea*
AREVA	*France*	**CRIEPI**	*Japan*	**GRS**	*Germany*
EDF SEPTEN/R&D	*France*	**KAERI**	*Korea*	**Zentech International Ltd**	*UK*
TWI	*UK*	**NPIC**	*China*	**SERCO**	*UK*
BE	*UK*	**RINPO**	*China*	**CSN**	*Spain*
INSPECTA	*Sweden*	**VEIKI Energia**	*Hungary*	**Tractebel**	*Belgium*
NRC	*USA*	**JRC Petten**	*Netherlands*		
BARC	*India*	**JAEA**	*Japan*		

2.2 Tasks presentation

Six tasks have been defined, which covers large number of configurations:

- Task 1: Elastic KI evaluation:
  - This first task focuses on KI compendia.
  - A first set of cases considered cracked pipes (with circumferential or longitudinal defect) under mechanical loadings (two loading conditions for each case).

- A last case considers a plate submitted to an exponential distribution for the nominal elastic stress, representative of a thermal loading.

- Task 2: J calculation for surface cracks in pipes
  - Only longitudinal or circumferential cracks in pipes are considered.
  - Three set of loading conditions have been defined: single mechanical loading, combined mechanical loadings and thermal loading (eventually combined with mechanical loading).
- Task 3: J calculation for circumferential through wall cracks in pipes
  - Only circumferential through wall cracks in pipes were considered.
  - Two sets of loading conditions have been defined: single mechanical loading, combined mechanical loadings.
- Task 4: J calculation for surface cracks in elbows
  - Only longitudinal or circumferential cracks in elbows were considered.
  - Three set of loading conditions have been defined: single mechanical loading, combined mechanical loadings and thermal loading (eventually combined with mechanical loading).
- Task 5: Particular cases
  - This task deals with particular geometries or loading conditions.
  - Four cases were initially proposed (imposed displacement loading condition, embedded cracks, underclad cracks, through clad cracks) but due to a lack of contribution only first and second sub-task were maintained.
- Task 6: J calculation in weld joints
  - The proposed cases focus on cracked pipes under mechanical loading conditions only. The case of residual stresses was not incorporated.
  - Discussion and conclusions.
  - This last step consists in a synthesis of the comparisons in order to identify, if possible, improvements of the different procedures.

All data required to perform these applications (geometries, material, loading conditions…) can be found in reference [6].

3. TASK1: ELASTIC KI EVALUATION

3.1 Introduction

The first task of KJ benchmark consists in a comparison of different procedures to evaluate the stress intensity factor K_I considering two main geometries: cracked (longitudinal or circumferential) pipe under mechanical loading and cracked plate under thermal loading (exponential distribution of elastic nominal stress). Several crack depths have been considered (4 for pipes, 8 for the plate, configurations recalled in Table 2). 23 contributions have been received, but only 11 were completed on all cases.

Figure 1. Figure 1: designation of defect type in studied configuration

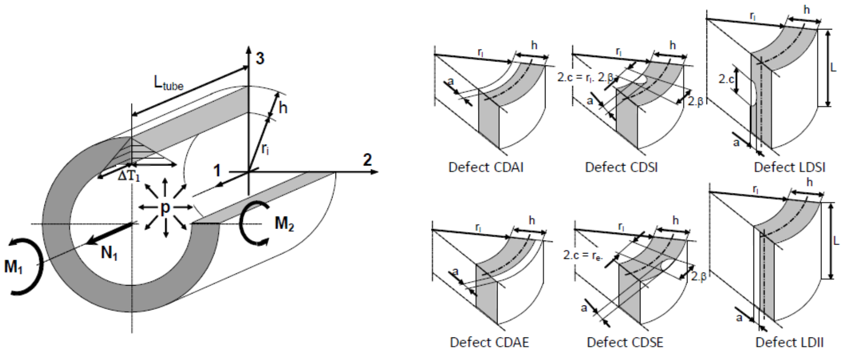

Table 2: Task 1 investigated configurations

GEOMETRY						
Case #	Geometry #	Defect	a/h	c/a	h (mm)	De (mm)
K1	PIPE 1	CDAI – circumferetial internal axysimetric	0.1 – 0.25 – 0.5 – 0.75	-	60	660
K2	PIPE 2	CDAE – circumferetial external axysimetric	0.1 – 0.25 – 0.5 – 0.75	-	60	660
K3	PIPE 3	CDSI – circumferetial internal semi-elliptical	0.1 – 0.25 – 0.5 – 0.75	3	60	660

GEOMETRY						
Case #	Geometry #	Defect	a/h	c/a	h (mm)	De (mm)
K4	PIPE 1	LDII – longitudinal internal infinite	0.1 – 0.25 – 0.5 – 0.75	-	60	660
K5	PIPE 2	LDSI – longitudinal internal semi-elliptical	0.1 – 0.25 – 0.5 – 0.75	3	60	660

Loading condition for pipe geometry	P (MPa)	M2 (N.mm)
C1	50	-
C2	50	6.0E+09

	Plate under thermal loading
Thickness h (mm)	10
Defect size a/h	0,1 to 0,8 (0,1 step)

Main answers were based on AFCEN codes (i.e. RCC-MR, RCC-MRx and RSE-M which share the same schemes for K_I and J evaluation) and ASME Section XI; these two codes covers 14 answers compared to a total of 23 received (see Figure 2 below, noticed that NB/T23012 refers to Chinese rules and SSM to K-solutions Handbook from Swedish Radiation Safety Authority [17]).

For K_I estimation, different steps have been performed leading to the final results presented in this report. It allowed some participants to correct such misunderstanding in loading (such as bending moment application or pressure on crack lips) or in geometrical consideration (such as crack shape for CDSI defect in pipe or nominal stresses compendia used).

Figure 2: Task 1 contributions

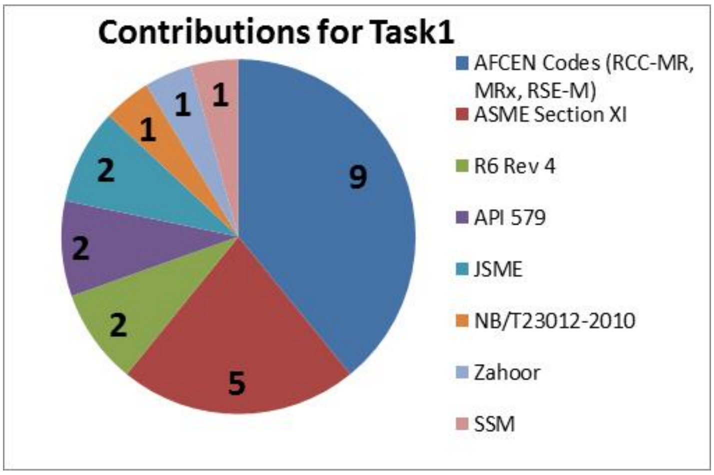

3.2 KI evaluation

First step in results analysis consisted in a comparison between participants using the same code. Considering level of contribution, Figure 3 to 6 plot the final (i.e. relative to last step) values of differences (error) (compared to finite element reference solution for the different defect type and depth, i.e. a/t ratio) for each configuration respectively for AFCEN code users, JSME, ASME and R6 users.

It can be noticed on Figure 3 that partners who used AFCEN code (except for one or two partners) a remarkable homogeneity of the results have been obtained. This result has been noticed since the initial step. Compared to FE reference solutions, the differences are mostly comprised between -10 and +10%.

Figure 3: AFCEN code users, comparison on pipe configurations

Figure 4: JSME users, comparison on pipe configurations

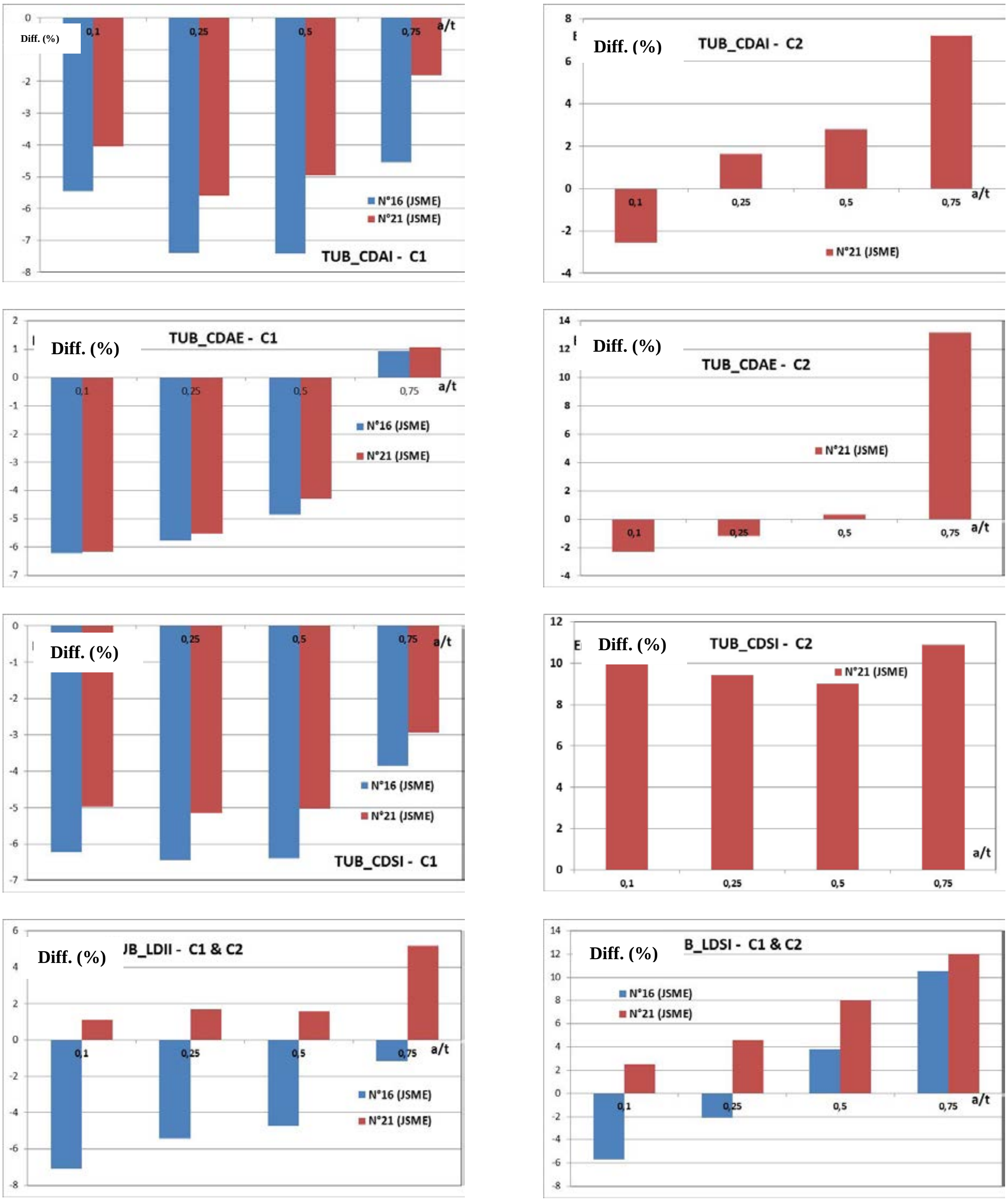

During the second step of task 1, one of the JSME users provided corrections (nominal stress consideration, ends caps effect for circumferential defect) and final results are homogeneous assuming partner 16 didn't provide results for some configuration submitted to circumferential defect under global bending.

As shown on Figure 5 below, ASME results remained difficult to explain: an important variability is obtained and results are in some cases far from reference solution.

Figure 5: ASME code users, comparison on pipe configurations

From the information received from ASME code users it has been noticed that, after the second step of task 1:

- Best results were obtained with partner 11 assuming:
  - Correction has been made for predictions relative to small defects but remained very pessimistic results for $a/t \geq 0.5$.
  - Unfortunately, no detail on the analysis has received.
- For Partner 17 it appears that :
  - Nominal stress calculations were comparable to AFCEN code results.
  - ASME Sect. XI – Appendix A has been used.
  - Results are correct for small defect in general.
- For Partner 10 :
  - ASME Sect. XI – Appendix C has been used.
  - Nevertheless, the nominal stresses are not consistent with other results.
  - Safety coefficient has been applied (2.7 on sm). Nevertheless, this loading amplification doesn't explain the discrepancies as if the initial result was divided by the safety coefficient, the FE results are then underestimated by more 50%.
- Considering Partner 5 :
  - ASME Sect. XI – Appendix C (Zahoor solution) has been used.
  - Only semi-elliptical defects (only 2 geometries on 5) have been considered.
  - No pressure on the crack lips has been taken into account.
  - Results were nevertheless correct.
- Considering Partner 7, no detailed information has been received.

No updated result has been sent by any partner using ASME code after second step of task 1.

For task 1, partner 1 contribution is based on K-solutions handbook available in SSM report [17]. Its results are plotted below with R6 users. Note that R6 users were not fully completed on all cases but it can be seen on Figure 6 that R6/SSM users provide correct estimation for the FE reference solution (more or less than max ± 10%). It must be mentioned that partner 1 hasn't applied pressure on crack faces (for internal pressure load) which can explain moderate negative differences.

Figure 6: SSM/R6 code users, comparison on pipe configurations

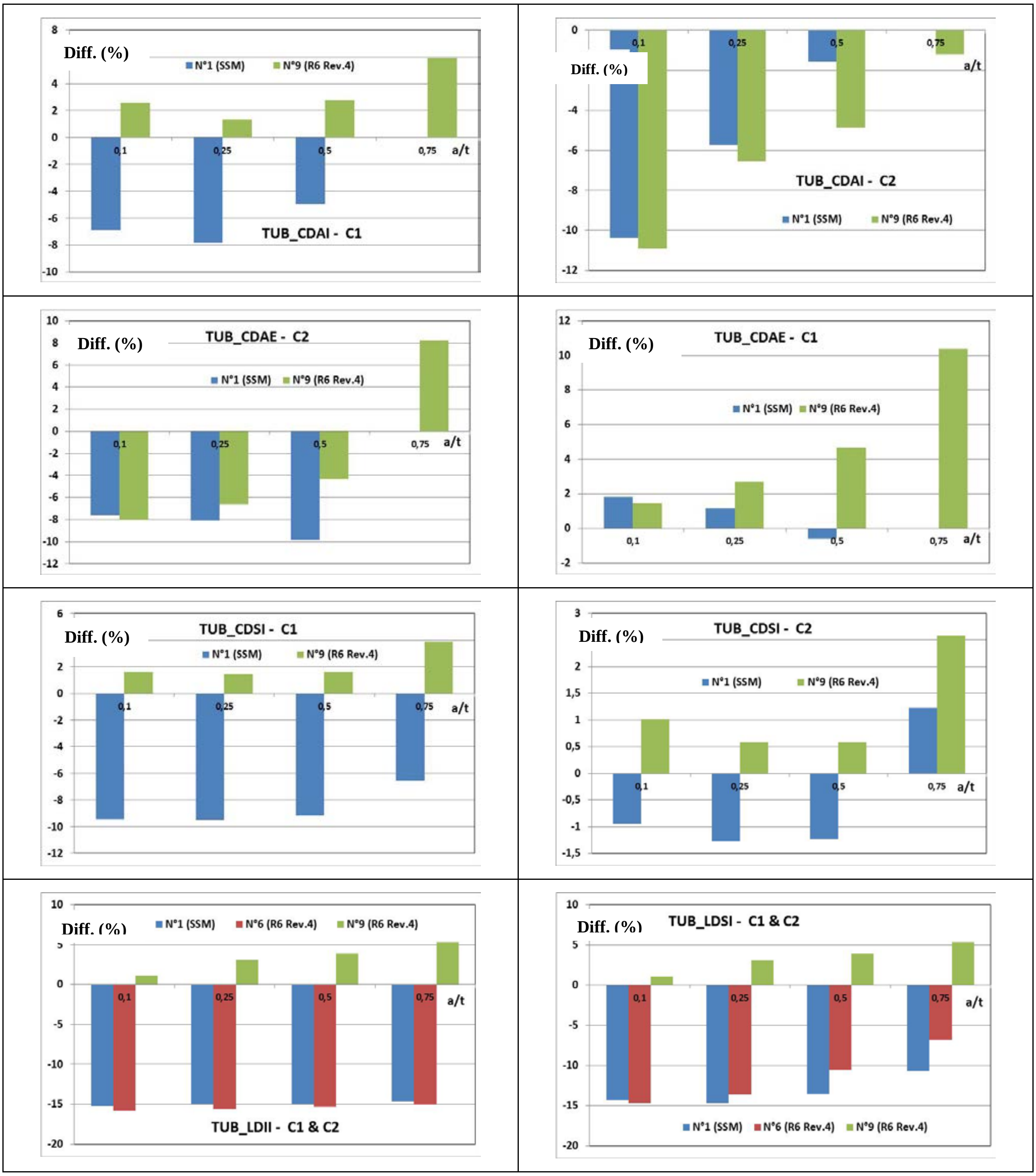

In order to get an idea of different codes accuracy, for each code, one representative partner has been then selected. Considering discrepancy for ASME users, the partner who provided the closest results to FE solution has been selected. Figure 7 sums up the results provided for task 1: for each kind of defect (CDAI, CDAE, CDSI, LDSI, LDII) and load history (C1 or C2) the differences are compared to finite elements solution and plotted as a function of ratio crack depth/thickness.

Figure 7: Percentage of differences compared to FE reference solution obtained by different codes application

Main conclusions on this task are the following:

- For cracked pipes, AFCEN codes, R6 and API provide in general relatively correct estimation in comparison to the FE reference solution (less than max ± 10%).
- JSME code provides also close results but under predicted often the FE solution, however the observed differences remained nevertheless less than -10%.
- Zahoor solution were in good agreement with all others results, but the difference with FE calculation was sometimes larger than the 4 first others codes.
- Solutions provided from participants using the ASME code remained problematic: an important variability has been obtained and results were besides far from FE reference solution. It is important to note that the available solutions are known: the discrepancies are mainly linked to code user errors. Some of them have been identified but the work requested to correct the predictions based on the ASME solution has not been performed.

The second part of task 1 dedicated to plate configuration is presented in Figure 8 to 10.

Figure 8 : Percentage of difference on plate configuration for AFCEN code users

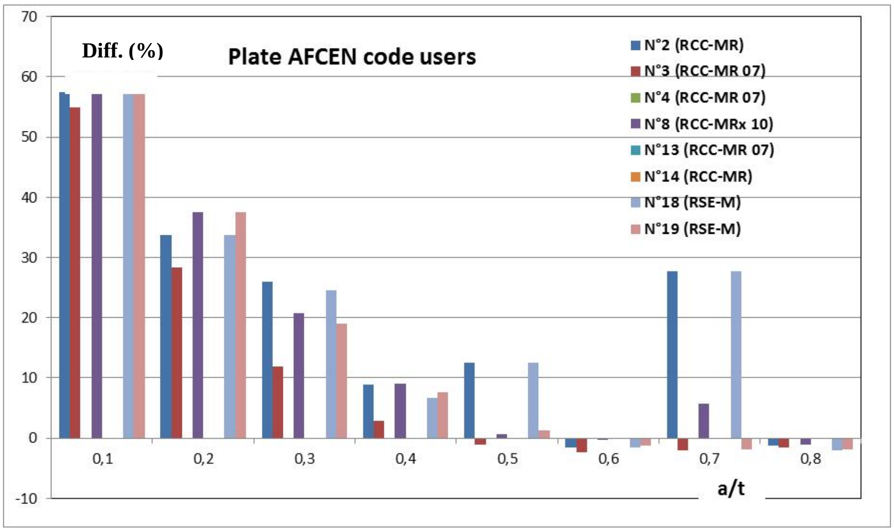

Figure 9: Percentage of difference on plate configuration for R6 users

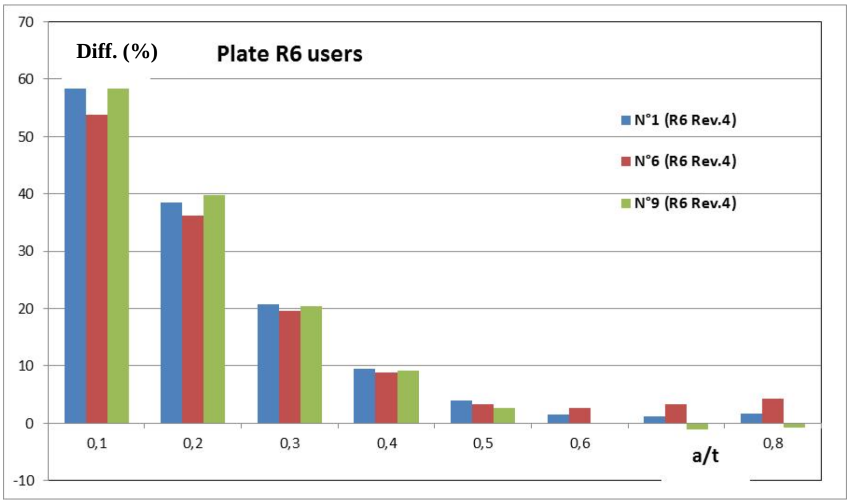

Figure 10: Percentage of difference on plate configuration for JSME users

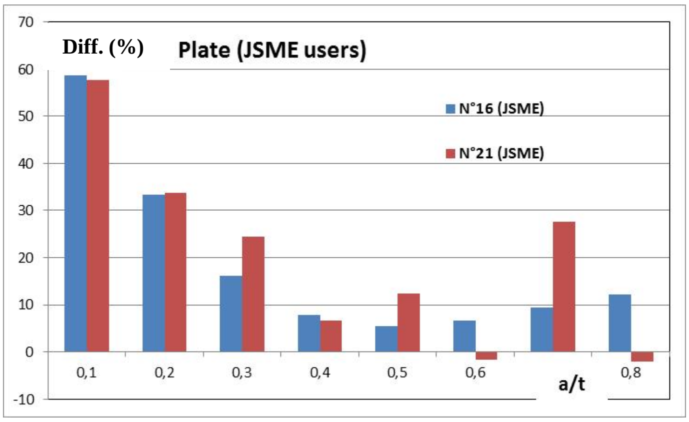

For the plate case with an exponential nominal elastic stress distribution representative to thermal loading, all codes provided very comparable results and all over predicted FE reference solution. Figures 8 and 9 show large relative difference for shallow cracks but small difference for deep cracks, which is most likely caused by small K-factors for shallow cracks, which lead large relative difference even with small absolute difference in value.

4. TASK 2 AND 3: J FOR SURFACE AND THROUGH WALL CRACKS IN PIPES

4.1 Introduction

Task 2 and 3 are quite similar and deal with J calculation for surface cracks (Task 2) and through wall cracks (Task 3) in pipes (see Figure 1 to recall defect designation of task 2):

- Task 2: 4 sub-tasks depending on type of defect and loading conditions have been defined :
  - Circumferential surface cracks submitted to mechanical loadings (P, M_2, M_1) (11 cases).
  - Longitudinal surface cracks submitted to mechanical loadings (P, M_2, M_1) (9 cases).
  - Elementary thermal loading i.e. imposed through thickness temperature variation with linear (ΔT_1) and quadratic component (ΔT_2) (7 longitudinal defects and 14 circumferential defects).
  - Combined mechanical plus thermal loading conditions (5 longitudinal defects and 6 circumferential defects).
  - Considering task 2, 14 contributions has been received.
- Task 3: 4 sub-tasks of pipes submitted to mechanical load have been considered. 9 partners sent a complete contribution for Task 3 based on analytical solution. Task 3 refers to through wall defect type described in Figure 11.

Figure 11: Geometrical description of CTR and LTR defect type used in task 3

Geometry of the defect CTR *(Circumferential through wall defect)* **Geometry of the defect** **2c : length of the defect (2c = 2β.rm)** **2β : angle of the defect (in radians), symmetrical position in relation to the bending plane**	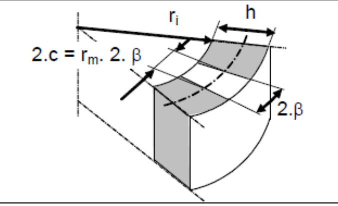
Geometry of the defect LTR *(Longitudinal through wall defect)* **Geometry of the defect** **2c** : length of the defect	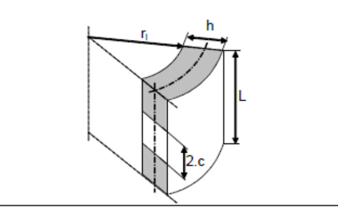

Figure 12: Task 2 and 3 contributions

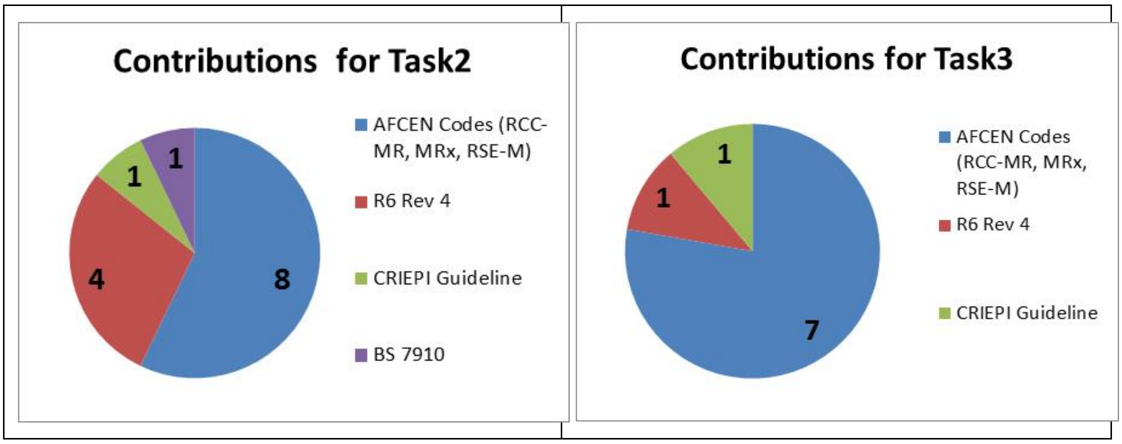

As shown in Figure 12, most partners used AFCEN and R6 codes for J estimation.

It must be mentioned that all results presented below, considering plasticity use AFCEN (RSE-M [1]) formulation of L_r parameter:

$$L_r = \sqrt{\left[\frac{3}{5}\cdot\frac{m_2}{q_m\cdot\mu_{em}\cdot\mu_t} + \sqrt{\left(\frac{n_1}{q_n\cdot\mu_{en}\cdot\mu_t}\right)^2 + \left(\frac{2}{5}\cdot\frac{m_2}{q_m\cdot\mu_{em}\cdot\mu_t}\right)^2}\right]^2 + \left[(1-\mu_{ti}).\frac{p}{\mu_{ep}}\right]^2 + \left[\frac{m_1}{q_n\cdot\mu_{en}}\right]^2} + \mu_{ti}\cdot\frac{p}{\mu_{ep}}$$

with $p = \frac{\sqrt{3}}{2}.\frac{P.R_m}{t.S_y}$ $n_1 = \frac{N_1}{2\pi.R_m.t.S_y}$ $m_1 = \frac{\sqrt{3}}{2}.\frac{M_1}{\pi.R_m^2.t.S_y}$ $m_2 = \frac{M_2}{4.R_m^2.t.S_y}$

4.2 Task 2 results: J for surface crack in pipes

For task 2 and task 3, results have been provided for J estimation at different level of load represented by parameter L_r ([1]). Comparison has been especially performed at two particular values of L_r, equal to 0.6 and $L_{r,max}$ but conclusions are the same, all curves presented below are plotted for $L_{r,max}$ values. Lr-max corresponds to a load level near plastic collapse. However, it should be noted that high load level $L_{r,max}$ for the evaluation of J could lead to very high values of J compared to the elastic solutions and further create large deviations from FEM solutions. For example using R6 or BS 7910, these solutions are known to be quite conservative for very high primary loads. This can be seen in some large positive relative differences in Figures 13-20.

Main conclusions on task 2 are summarised below:

- ***For mechanical loading*** (see illustration on Figure 13 and 14): AFCEN codes lead to homogeneous results except isolated singular error (such as partner 20 on case C4 on Figure 13). Considering R6 users, it seems difficult to give a global trend because of important differences between the sets of results (Figure 15). It can therefore be noticed that only two R6 users sent results for longitudinal defect (partner 6 and 9, see Figure 16) which are far below FE solution (one order of magnitude at $L_{r,max}$ i.e. maximum load level considering AFCEN code notation). Note that BS 7910 user provides such conservative values that he could not provide values for maximum level of load (probably due to an out of range of stress/strain curve given for the analysis).

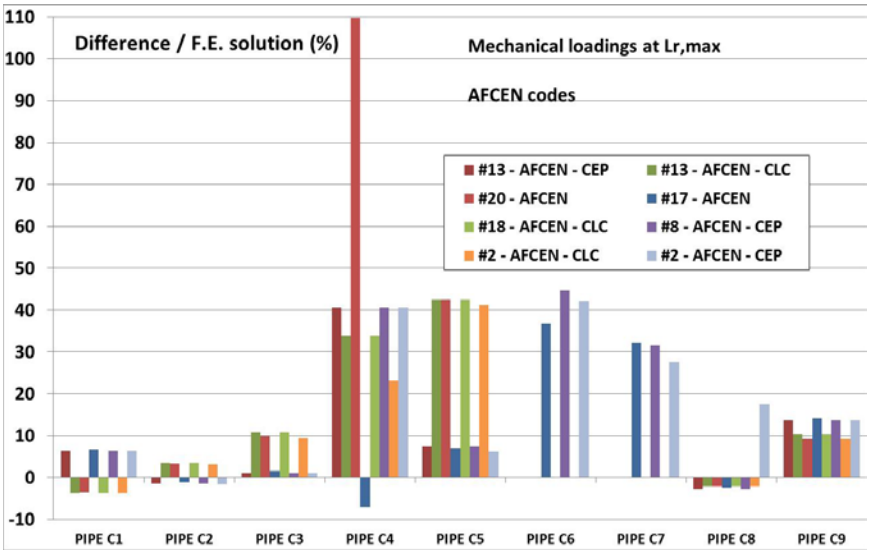

Figure 13: AFCEN users results compared to FE reference for circumferential defect in pipe under mechanical load (at maximum level $L_{r,max}$)

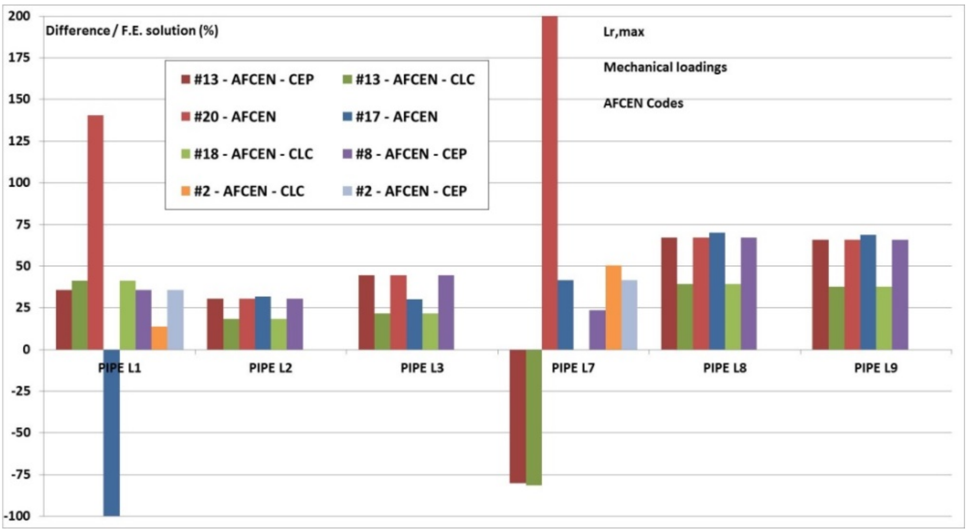

Figure 14: AFCEN users results compared to FE reference for longitudinal defect in pipe under mechanical load (at maximum level $L_{r,max}$)

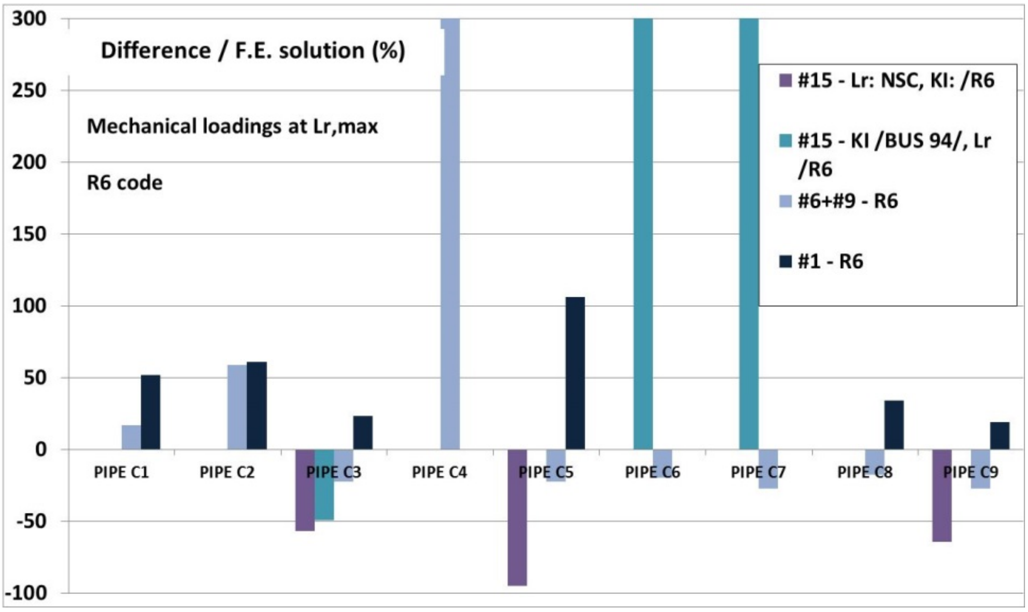

Figure 15: R6 users results compared to FE reference for circumferential defect in pipe under mechanical load (at maximum level $L_{r,max}$)

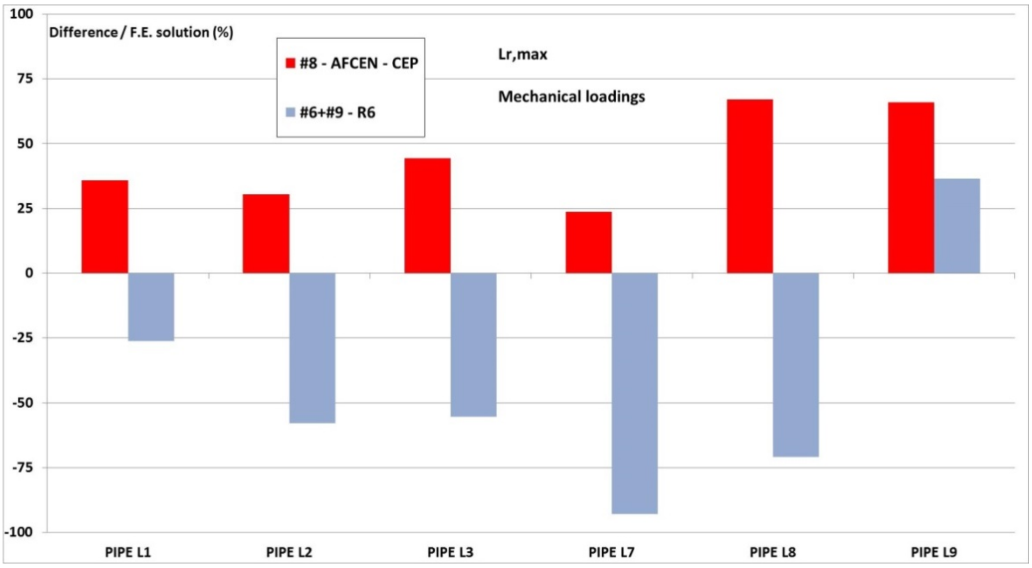

Figure 16: R6 and representative AFCEN users results compared to FE reference for longitudinal defect in pipe under mechanical load (at maximum level $L_{r,max}$)

- ***For pure thermal loading***: AFCEN codes provided in general homogeneous (except partner 17) and slight conservative prediction for loading conditions relatives to linear temperature gradient (ΔT_1) (configuration C12 to C16 on Figure 17), assuming different option are available. Some discrepancies nevertheless are shown on Figure 17 between AFCEN code users for other configurations including quadratic contribution in thermal load (ΔT_2): in fact, it appears that most partners didn't take this contribution into account in elastic part estimation (K_I), leading to a underestimation of J, whereas the method is available in AFCEN code (as partner 8 did).

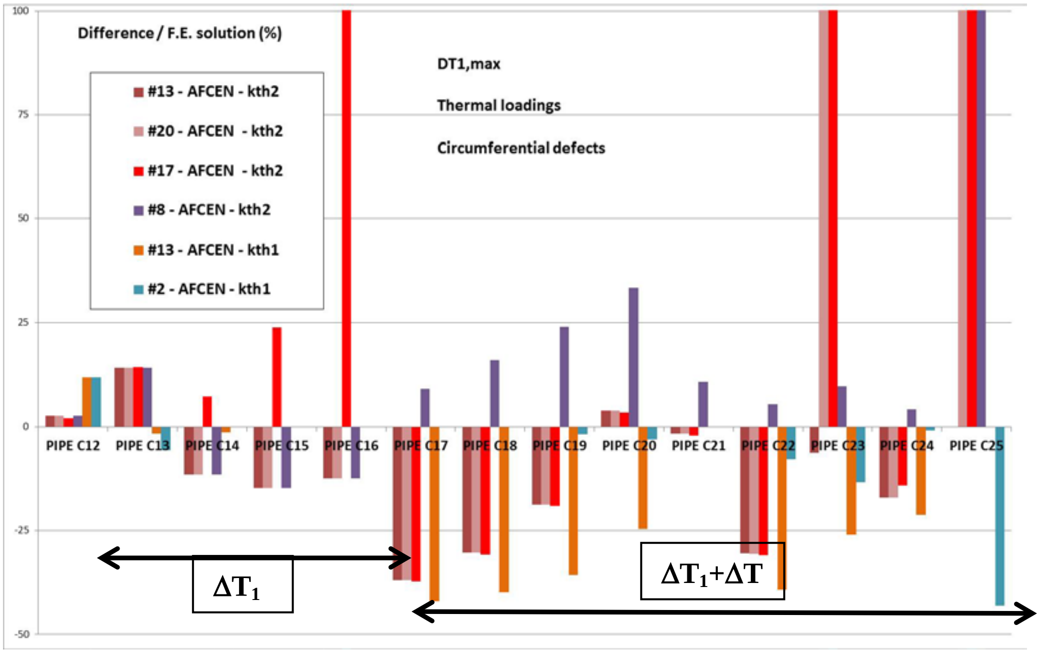

Figure 17: AFCEN code user's results on J estimation for circumferential defect in pipe under thermal loading

R6 code (applied considering the elastic solution for J) provides more conservative results. Nevertheless BS 7910:2005 results are the most over-conservative (probably linked to a user error). Figure 18 gives an overview on this.

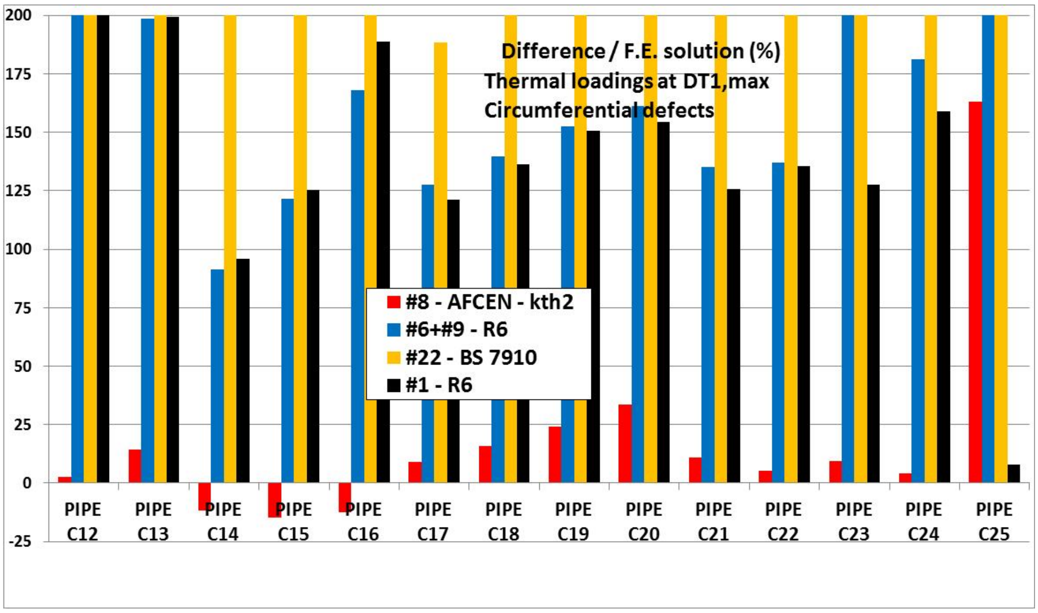

Figure 18: Comparison between different codes used for J estimation in pipes with a circumferential defect under thermal loading

- ***For combined thermal plus mechanical loading***: conclusions are the same than for pure thermal loading that means assuming that discrepancies due to ΔT_2 shown in Figure 17 may be offset by initial mechanical contribution. Figure 19 and 20 show the results obtained at maximum level of load for AFCEN code users, which are then compared by the one's provided by R6 users.

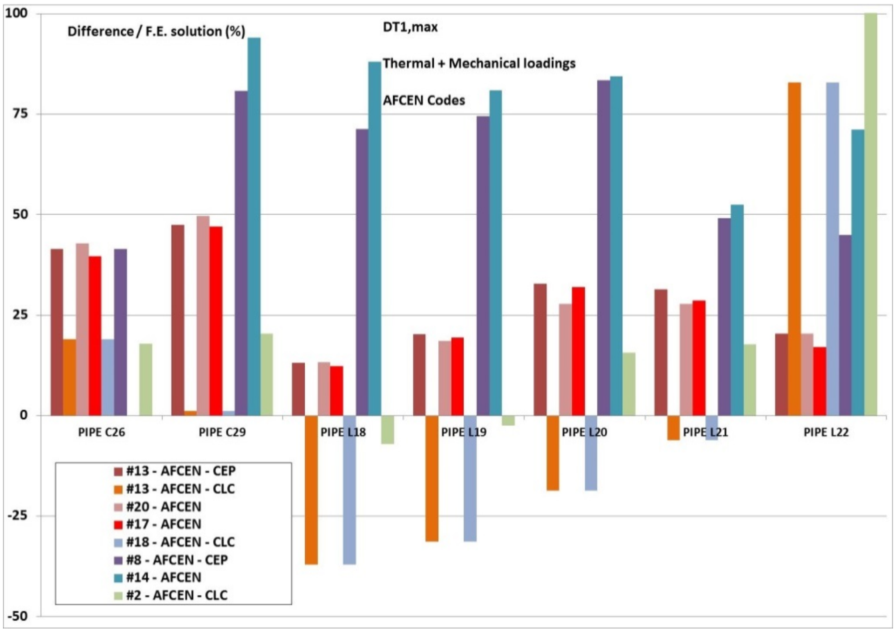

Figure 19: AFCEN code users results on J estimation for circumferential defect in pipe under combined mechanical (P, P+N_1 or M_2) plus thermal loading (ΔT_1 or $\Delta T_1 + \Delta T_2$)

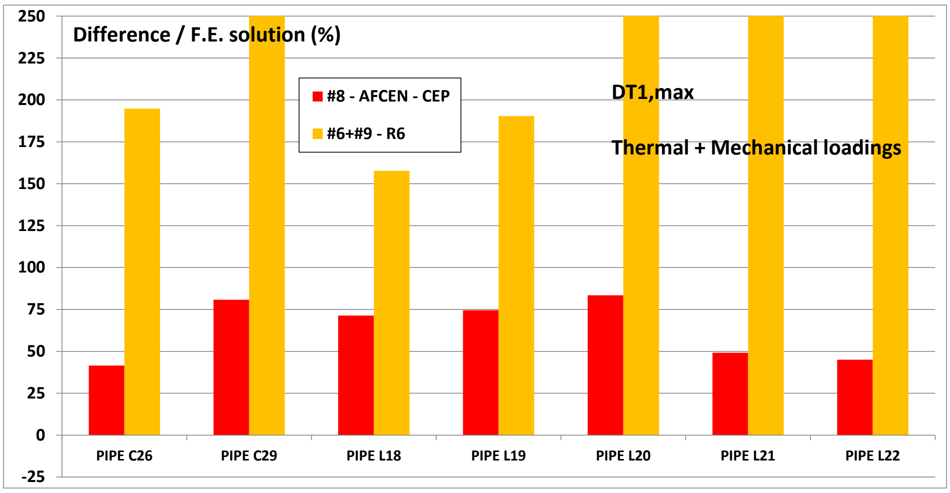

Figure 20: Comparison between representative AFCEN code user and R6 users for J estimation in pipes with a circumferential (C) or longitudinal (L) defect under mechanical plus thermal loading

4.3 Task 3 results J for through wall crack in pipes

First of all Figure 21 compares the result (in terms of difference between analytical evaluation and FE reference solution at the maximum load level $L_{r,\,max}$) between AFCEN users themselves.

Considering a good homogeneity of the AFCEN code results is observed, Figure 22 then plotted the result of one representative AFCEN user (#8) and other codes. Only partner 3 provided “singular” results. Besides it could be noticed than R6 and AFCEN codes lead to comparable results whereas CRIEPI Guideline results are very low compared to the other ones.

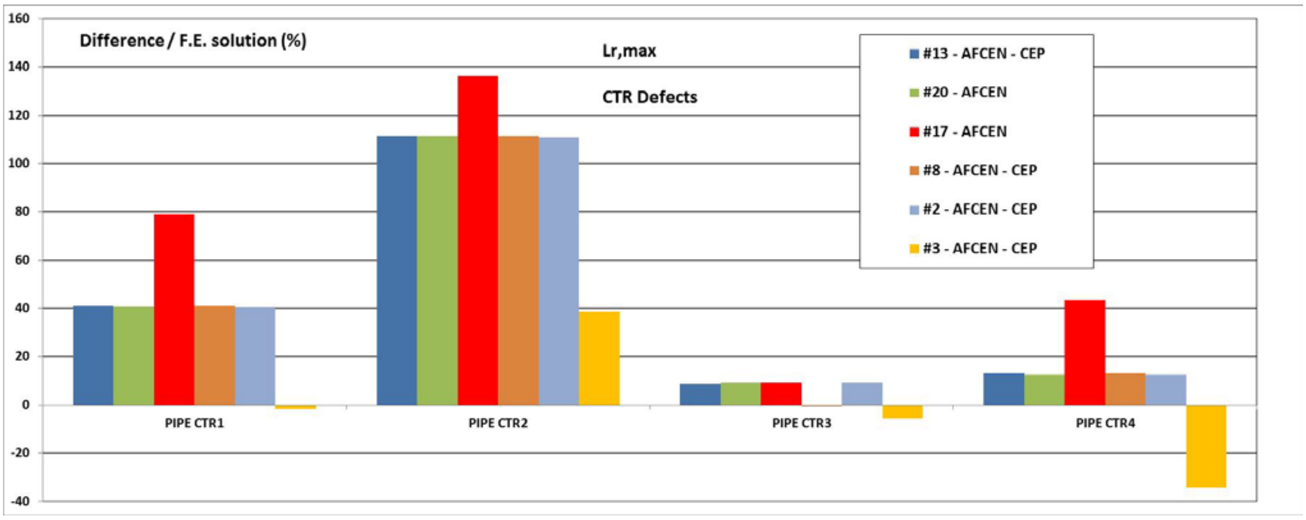

Figure 21: AFCEN code user's results on CTR defect

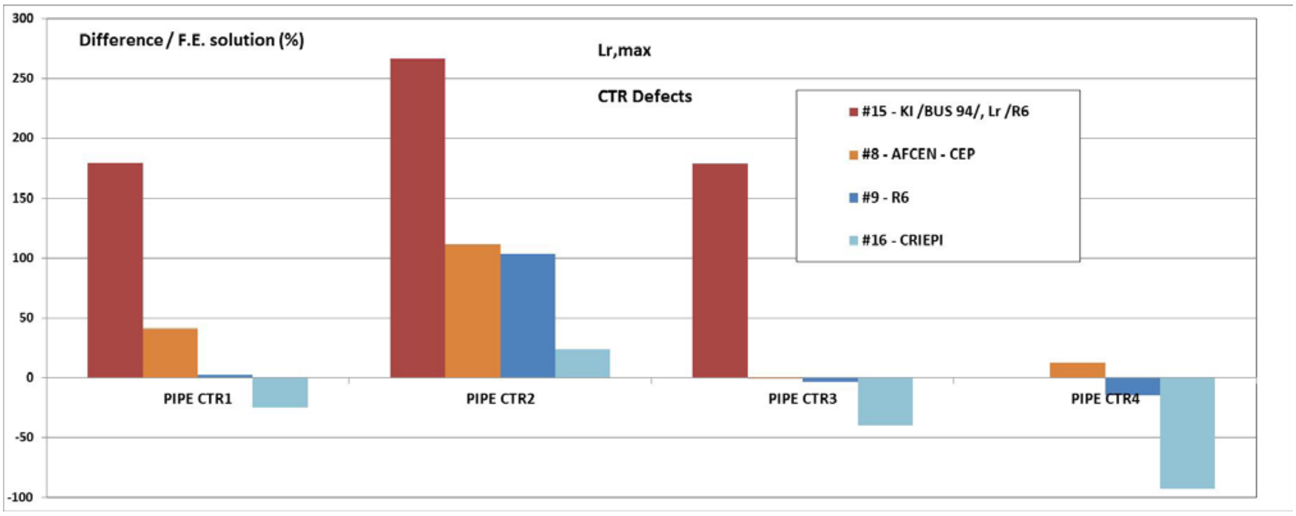

Figure 22: comparison between representative AFCEN code users and R6/CRIEPI users

5. TASK 4 – CRACKED ELBOWS

5.1 Introduction

Task 4 focused on the analytical calculation of the J parameter for circumferential or longitudinal crack in elbows submitted to mechanical, thermal or combined loadings. Elbow configurations introduced additional difficulties due to the number of geometrical parameters to take into account (see Figure 23), which have as an example an impact on the nominal stresses to take into account in the analysis, and as an consequence are not actually as well studied as pipe configuration in different codes and standards. Finally, for this task, most of the contribution relies on AFCEN codes (RCC-MRx or RSE-M which in fact share the same schemes) or on finite element computations even if it's initially out of the scope of the benchmark (which focus on analytical method).

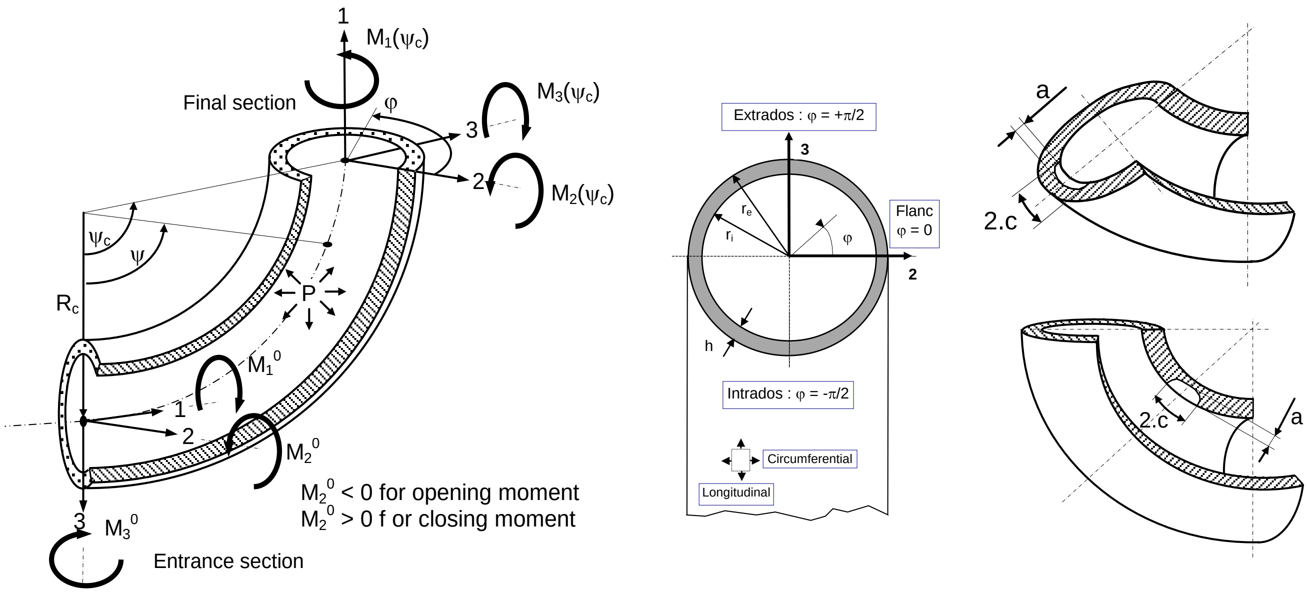

Figure 23: Geometrical description of task 4 elbow cases

Table 3: Elbows configuration considered in task 4

		Load							
		Single mechanical			Combined mechanical			With thermal	
		P	M2	M3	P+M2	M2+M3	M1+M3	deltaT	M2+deltaT
Defect type		1			1				
Circumferential	CDAI	1		1					
9 cases	CDSI					1			1
longitudinal	LDII	1	1						
8 cases	LDSI	1			1	1		1	1
	LDSE		1						

Eight partners provided results using AFCEN codes or finite elements calculations:

- Korea University
- KAERI
- JRC
- RINPO
- BARC
- EDF R&D
- EDF SEPTEN
- CEA

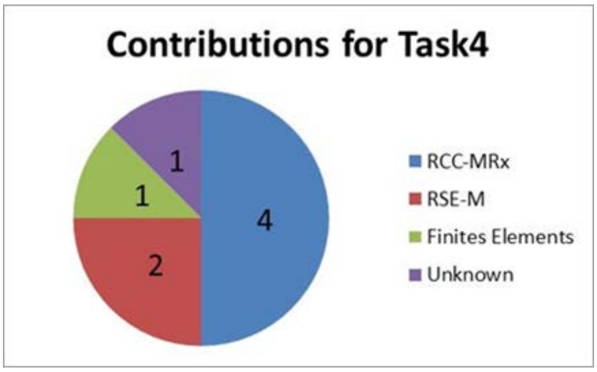

Figure 24: Task 4 contributions

It should be noticed that even the FE results provided by the partner 14 presented important differences with CEA reference results, which were already benchmarked between EDF, AREVA and CEA. As it can be seen through the number of contributions on this task, its difficulty appears to be "a bit reluctant" not only from an analytical point of view but also for FE calculations which are also not so easy to correctly perform (many risk of errors on boundary conditions, loading applications, minimal length of straight section to consider and so on…). This point confirms the interest for a potential FE calculation benchmark in the future. At this step, these FE results are not considered in the following analysis.

As elastic-plastic J calculation is based on two elements (elastic solution J_{el} and the elastic-plastic correction) the analysis is divided into two phases: the first one focus on elastic value of J and the on the elastic-plastic correction which in fact consists in AFCEN codes in a plastic amplification of the elastic term of J.

Note that a mistake on the bending moment sign was introduced in the first version of the benchmark. As all partners had not the possibility to revise their proposition, the concerned cases have been excluded from the analysis.

5.2 Elastic value of J

5.2.1 Mechanical loads

Figure 25 presents a synthesis of the different results, considering, for each case and each partner, the difference between the benchmarked CEA FE reference cases. Differences refer to the maximal loading condition ($L_{r,max}$) for each case, but conclusions are the same for all loading levels.

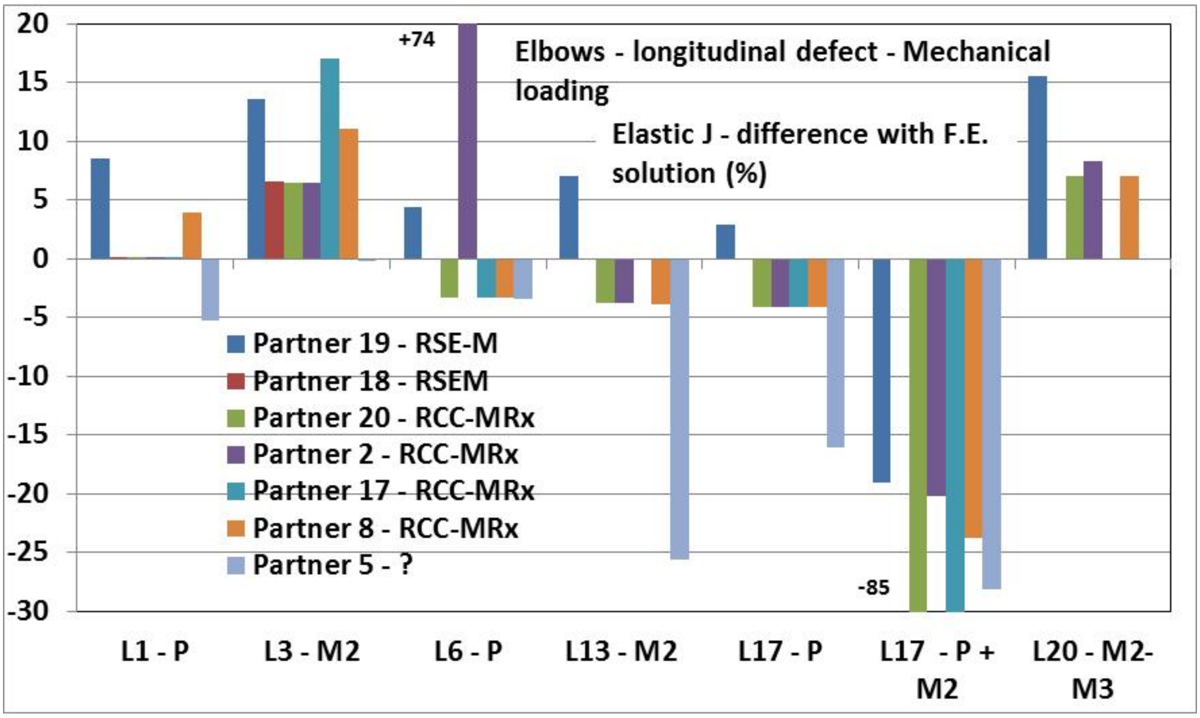

Figure 25: Comparison between the FE reference solution for the elastic value of J and the analytical results for each partner and each case at $L_{r,\,max}$ for longitudinal defects.

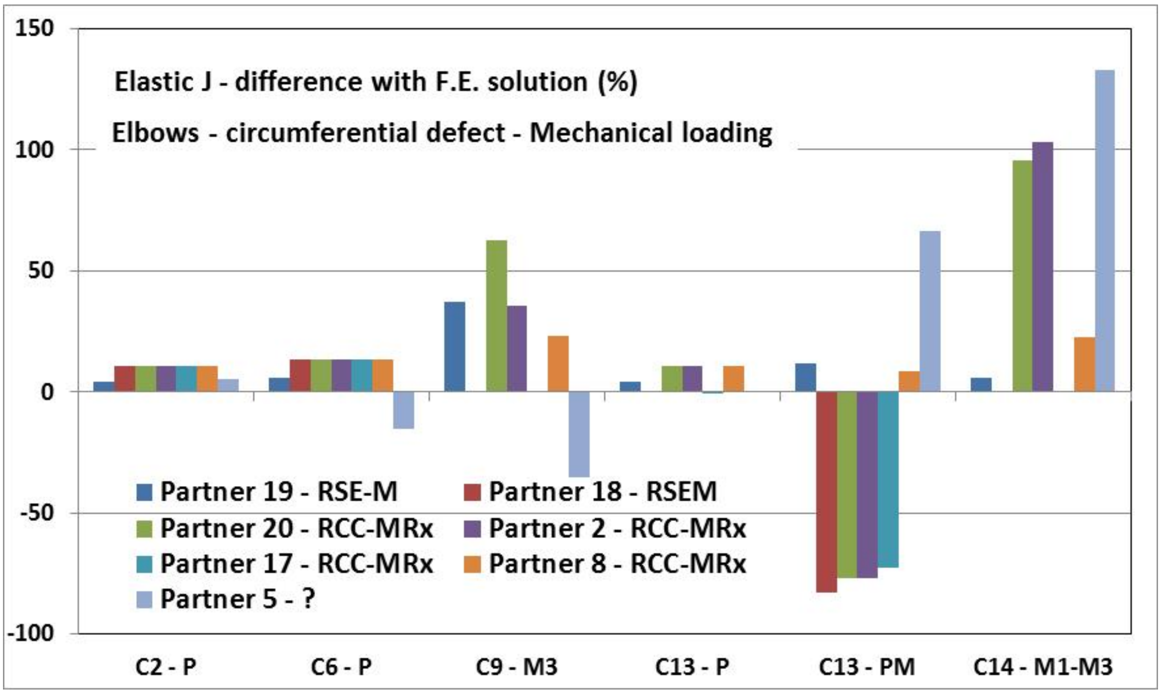

Figure 26: Comparison between the FE reference solution for the elastic value of J and the analytical results for each partner and each case at $L_{r,\,max}$ for circumferential defects.

For mechanical load, considering circumferential or longitudinal defects, results are globally homogeneous and J values are well predicted under pressure loading conditions, analytical results are mostly comparable to FE results (in general less than 5%). Nevertheless when load implies bending and torsion moment, more discrepancy especially in the cases of circumferential defect are shown. In such cases J may be largely over or under predicted (except partners 8 and 19) which may be due to the section considered (median one instead of entrance). Today, it is assumed that other partners than 8 and 19 have considered a defect in the median section, as for longitudinal defects: higher values (in absolute value) of J are in general observed in this section, which is consistent with the received results.

As a general remark, it should be noticed that, considering for AFCEN codes, the methodology is based on the calculation of the nominal elastic stresses in the elbows and the use of the influence coefficient of the cracked pipes with the same defect: this method is off course less accurate than an approach using dedicated compendia of influence coefficients. It would be interesting to have more information on the elastic nominal stresses calculation and the obtained results by each partner.

Particular cases are nevertheless observed, which are probably due to user's error:

- Partner 2 (used AFCEN code) for the case L6, C14.
- Partner 20 (used AFCEN code) for case L17, C14.

5.2.2 Thermal and combined loads

Under thermal and combined load, a good homogeneity of the results is obtained for each case and the reference elastic solution is underestimated by all the partners (see Figure 27). It is due to the fact that only linear through thickness temperature variation is proposed in the J elastic solution, whereas the considered cases correspond to a non-linear variation. This point shall be improved in the future to be able to deal with these configurations.

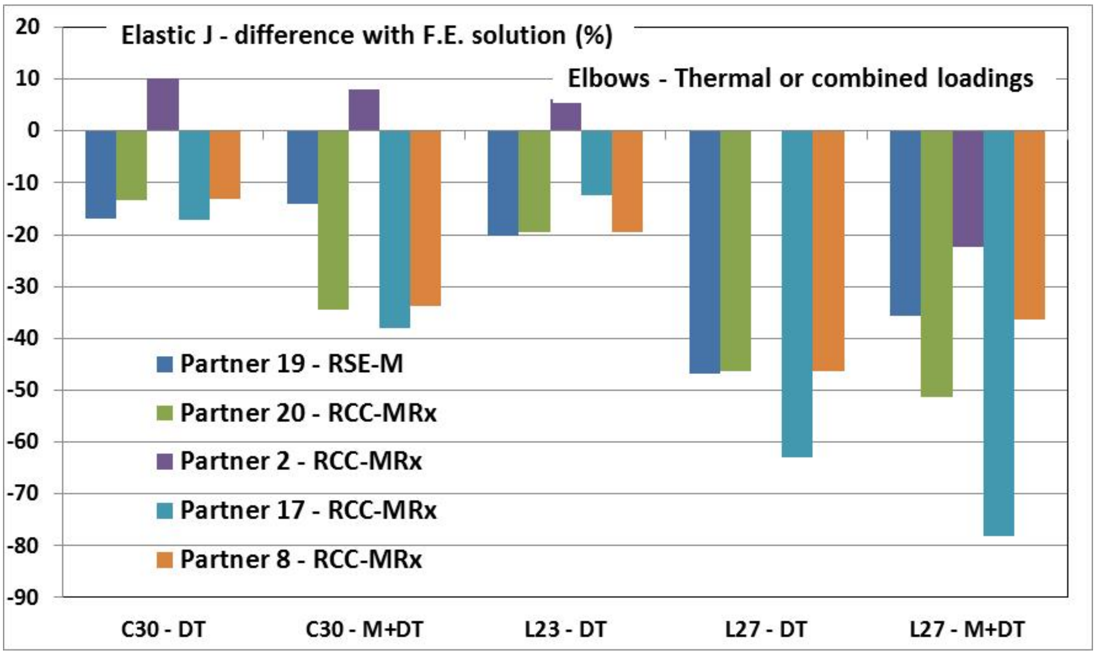

Figure 27: Comparison between the FE reference solution for the elastic value of J and the analytical results for each partner and each case at ΔT_{max} for thermal loads.

5.3 Elastic-plastic correction

This paragraph focuses on the elastic-plastic correction, i.e. the ratio J/J_{el} in order to reduce the impact of estimation of J_{el} on potential discrepancy. On following Figures for this part, first drawbar represents the amplification given by the reference finite element calculation at maximum level of load (conclusions are the same for lower values).

5.3.1 Mechanical loads

For mechanical load, results are good agreement considering that two groups can be observed, due to the option (CEP or CLC options available in AFCEN codes) selected by the partner. As for elastic value, a little more variability is obtained for bending moment compared to pressure load. As previously mentioned FE results from partner 14 remains unexplained.

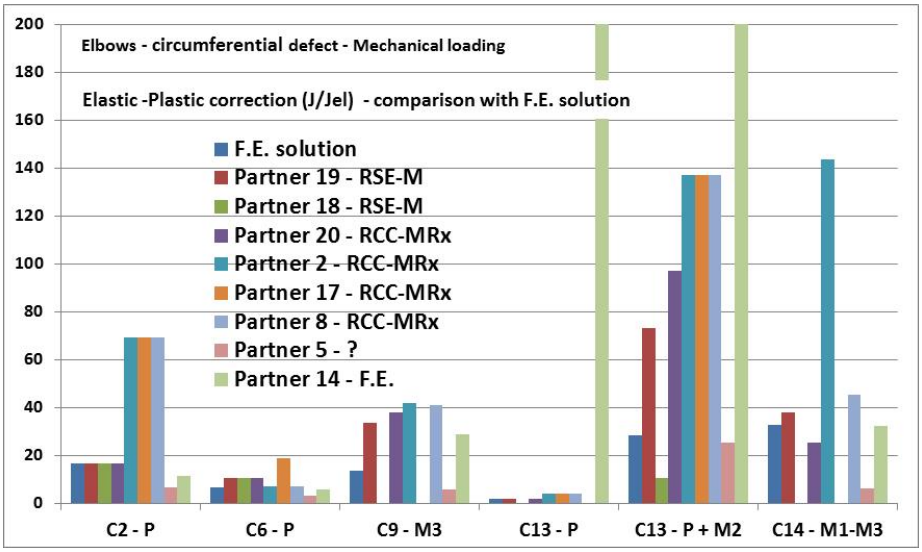

Figure 28: Elastic-plastic amplification at maximum level of load for elbow with circumferential defect under mechanicals loading

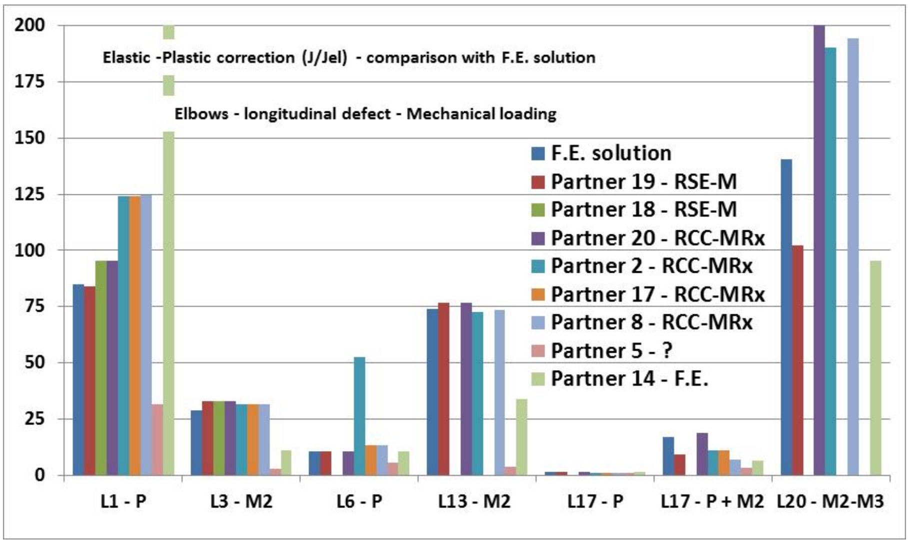

Figure 29: Elastic-plastic amplification at maximum level of load for elbow with longitudinal defect under mechanicals loading

5.3.2 Thermal and combined loads

Figure 30 directly compares the FE value of the elastic-plastic correction for each case with the analytical solutions, for the maximal thermal loading condition (the conclusions are unchanged for lower loading condition).

Note that all results presented here have been produced using the AFCEN codes. Partners 17 and 20 provided particular results for combined loadings. The other results present a good homogeneity and are close to the FE solution (first drawbar).

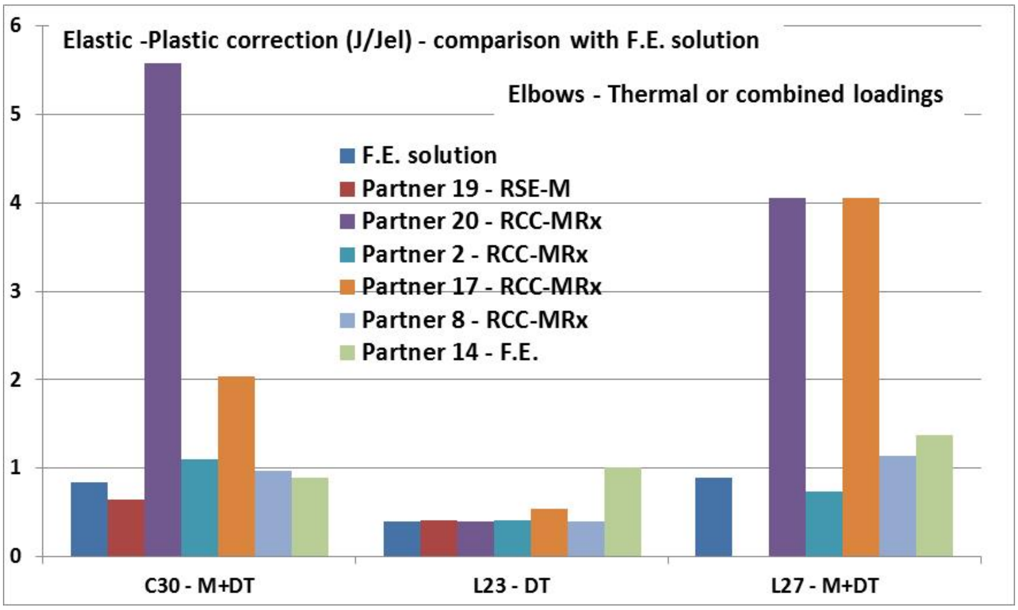

Figure 30: Comparison between the FE reference solution for the elastic-plastic correction and the analytical results for each partner and each case at $L_{r,max}$ for thermal or combined loadings.

6. TASK 5 – PARTICULAR CASES

This task was initially divided in 4 sub-tasks but considering only 2 FE contributions were received for the 2 last, the two first sub-tasks only were threated. They deal with:

- Estimation of elastic-plastic values of J for a cracked pipe submitted to an imposed displacement.
- Estimation of elastic stress intensity factor K_I in pipes containing embedded crack.

6.1 imposed displacement loading condition

This first particular case concerns a cracked pipe. The considered defect consists in a circumferential axisymmetric one with a depth equal to 2.5 mm (for a thickness of 10 mm). One section is embedded whereas the opposite section is submitted to a uniform axial displacement of 0.645 mm.

4 partners provided results:

- Korea University
- KAERI
- GDF-SUEZ
- CEA

Only one partner on this four provided analytical solution based on RCC-MRx procedure, all others used FE calculations.

Figure 31 compares the different results. Partners 8 and 3 get similar FE results. Partner 14 is a little bit higher, but it is suspected that there is a mistake in the displacements definition: in fact if the displacement is multiplied by two, the impact on the curve makes it fits the ones provided by partners 8 and 3.

Partner 17 provided corrected results in a second step assuming he did the same mistake but if the general shape of the curve is similar, J values stay nevertheless too high. Looking at Figure 32 focusing on elastic values of J, J_{el}, it seems that another problem occurred, maybe in the crack shape definition.

The analytical solution of the RCC-MRx appears to be a conservative but reasonable solution. The higher difference is observed at the beginning of the plasticity. When the plasticity is fully developed, the analytical solution seems to get closer to the FE solution.

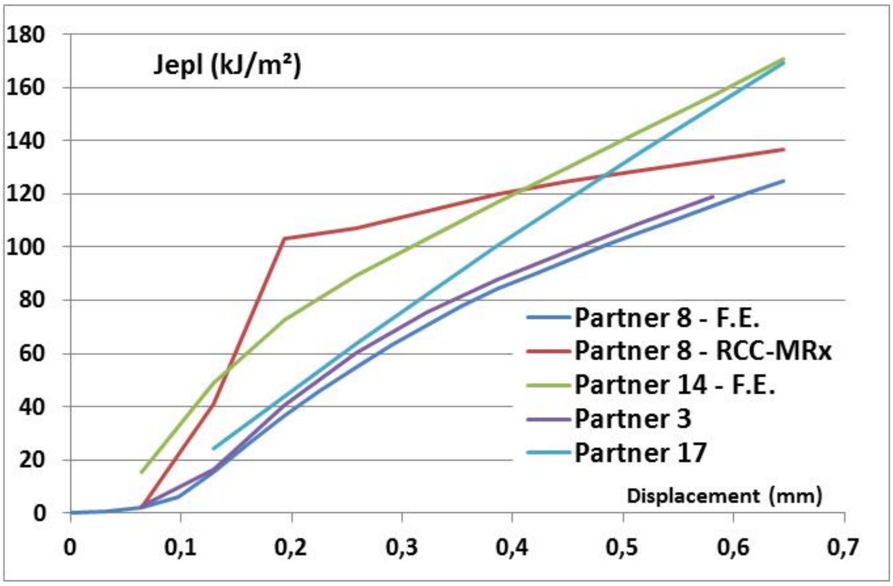

Figure 31: Comparison of Jepl values provided for pipe under imposed displacement

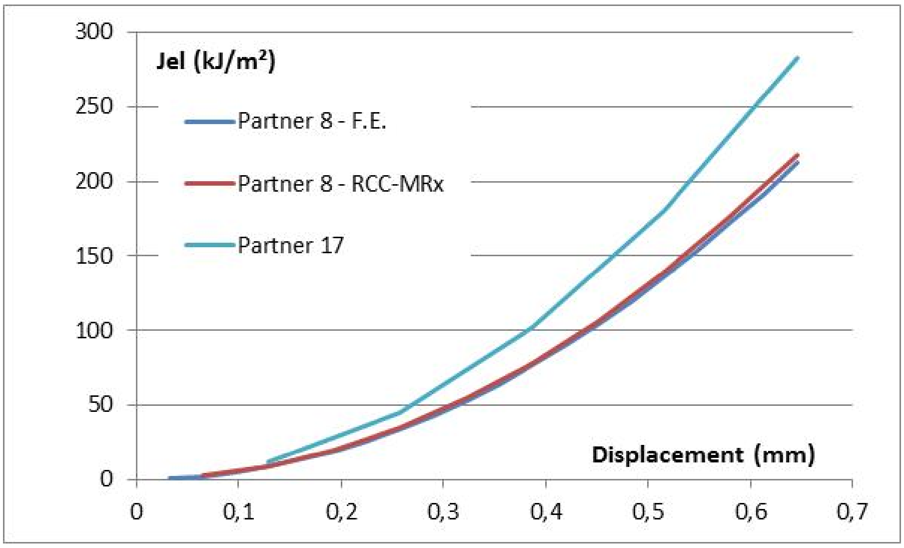

Figure 32: Comparison of Jel values provided for pipe under imposed displacement for partner 8 and 17

6.2 Plate with embedded defect

The second sub-task focused on the calculation of the elastic value of J parameter for a plate (thickness h equal to 10 mm and width 2b equal to 350 mm) submitted to an axial load and a bending moment, and containing an embedded elliptical defect. 20 cases have been investigated, depending on crack size (see Table 4).

Geometrical description of such defect is recalled in Figure 33.

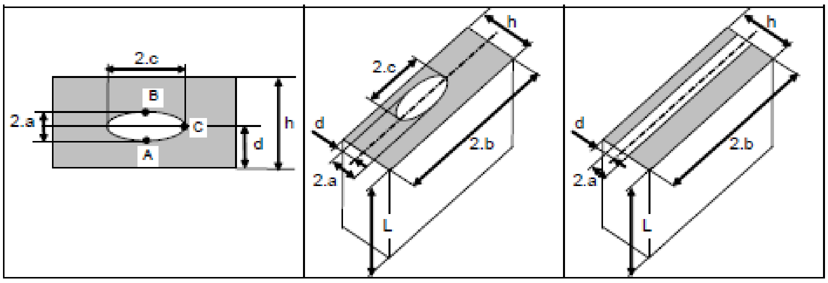

Figure 33: embedded defect geometries

Table 4: embedded defect sizes investigated

2a/h	0.1	0.5
d/h	0.1, 0.3, 0.5	0.3, 0.5
c/a	1, 3, 6, ∞	

Four partners provided results:

- Korea University
- KAERI
- GDF-SUEZ
- CEA

Partner 14 provided FE calculation results whereas other partners used the analytical solution proposed in the appendix A16 of the RCC-MRx code. Results are plotted on Figure 34 in terms of K_I values.

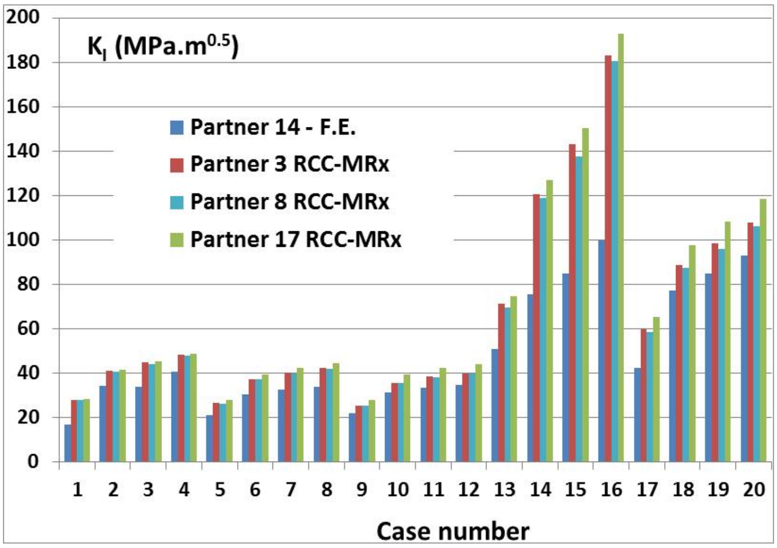

Figure 34: Comparison between the FE solution for the elastic value of K_I (provided by the partner 14) and the analytical results for each partner and each case.

Globally, the three partners using the AFCEN codes provided similar results. It has been noticed that partner 17 get slightly higher values, whereas the difference between the results of the partners 8 and 3 are within 2% (except the cases 15 and 19 where differences are a bit higher). In fact, in the 2010 edition of the appendix A16 of the RC-MRx, the chapter on the related compendia was incomplete and didn't provide details on the nominal elastic stresses. It can be understood in the corresponding text that these stresses can be estimated using the same solution for surface crack. In fact, it is not the case (the last version of the appendix has been completed): for the elastic stresses, the linear representation of the related distribution is centred on the middle of the crack. Finally it has been possible to reproduce the results of partner 17 using the elastic stresses for surface crack: this result put forward an inaccuracy of the 2010 edition of the RCC-MRx code which has been modified in the last update.

7. TASK 6 – CONSEQUENCES OF WELDS

7.1 Task presentation

Task 6 focused on cases with a circumferential (semi-elliptical or axisymetrical) crack in a weld. The aim was to investigate solutions available to take into account mismatch effect on the J calculation. No residual stresses have been considered in the FE reference calculations, and there was no recommendation on this point in benchmark description but one partner (partner 6) used R6 Section IV compendium to introduce RS profile.

Figure 35 and Table 5 recall the configuration investigated. Note that only one defect position of Figure 35, where the defect is located in the middle of the weld (position 1), was considered in the benchmark.

Regarding loading conditions, only the mechanical load (axial, internal pressure and bending moment) has been considered.

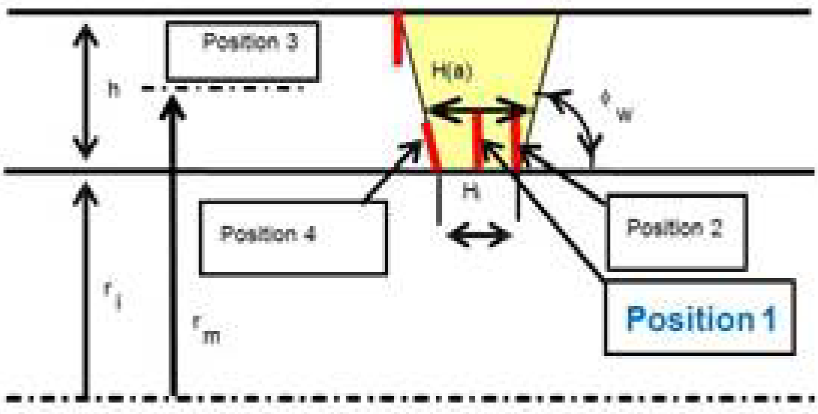

Figure 35: Weld configuration considered in task 6

Table 5: description of defect type (located in position 1) investigated

Config	Defect type	Weld angle	a/h	Defect length/depth	Mismatch
W2	CDAI	90	0,25		1,5 (Rambert-Osgood)
W5	CDAI	90	0,25		2,3 (Rambert-Osgood)
W6	CDAI	90	0,0625		2,3 (Rambert-Osgood)
W8	CDAI	60	0,25		2,3 (Rambert-Osgood)
W9	CDAI	60	0,25		2,3 (Bilinear)
W11	CDSI	60	0,0625	2	2,3 (Rambert-Osgood)
W13	CDSI	60	0,25	2	2,3 (Rambert-Osgood)
W14	CDSI	60	0,25	2	2,3 (Rambert-Osgood)

Note that, due to the complexity of this task, the number of configuration has been reduced (compared to the initial work planned in the frame of the benchmark) but only 3 partners provided results on all 8 cases.

Six partners provided results:

- Korea University
- KAERI
- AREVA
- AMEC
- GRS
- CEA

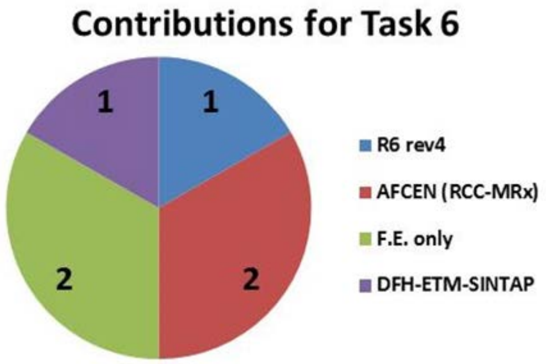

Figure 36: Task 6 contributions

Partners 14 and 17 provided FE results only. These calculations will be then compared to the CEA reference FE calculation.

Partners 8 and 13 used the appendix A16 of RCC-MRx approach based on the definition of an equivalent material: the case is then analysed as a homogeneous case, with a tensile curve deduced from the original tensile curves defined for the base metal and the weld.

Partner 6 used R6 approach. Nevertheless, the mismatch effect was not considered, whereas R6 rules include a similar method than the RCC-MRx code. Partner 6 used the base metal properties which lead here to conservative results as the weld is overmatched. Also, he considered residual stresses, as secondary stresses, with a reference field defined in the R6 code. Partner 15 used the DFH-ETM-SINTAP (DES) approach for mismatch welds, with the specific limit load formulation for weld joints ETM.

7.2 Comparison of results

Figure 37 shows the results obtained at higher level of load (Lr_max) on 8 cases. Green and red lines correspond respectively to exact solution ($J=J_{F.E.\ ref}$) and to a two ratio ($J=2.\ J_{F.E.\ ref}$).

AFCEN code users provided exactly the same results on both CEP and CLC option, which appears to be conservative on all 8 cases. It can be noticed that CLC option seems to give closer results on the studied cases but there is too few configurations to generalise this point. Besides, for this task which remained complex even in terms of analytical method, it appears that AFCEN codes users performed both their analysis with a free distributed tool, call MJSAM, developed and validated by CEA, and which contains all analytical methods described in RCC-MRx A16 appendix. It necessarily helped to reduce the discrepancy between AFCEN code users.

R6 user is also conservative on all cases except on W9 which seems to conduct to large discrepancy, keeping in mind concerned partner took into account residual stresses. DES user provided singular results (very low value of J) on both cases W8 and W9. It can be noticed on Figure 38 that there is even no satisfactory agreement on finite element computations performed on these cases. Except these configurations, results range (in terms of elastic-plastic value of J at maximum level of load) between the reference solution and twice this reference value.

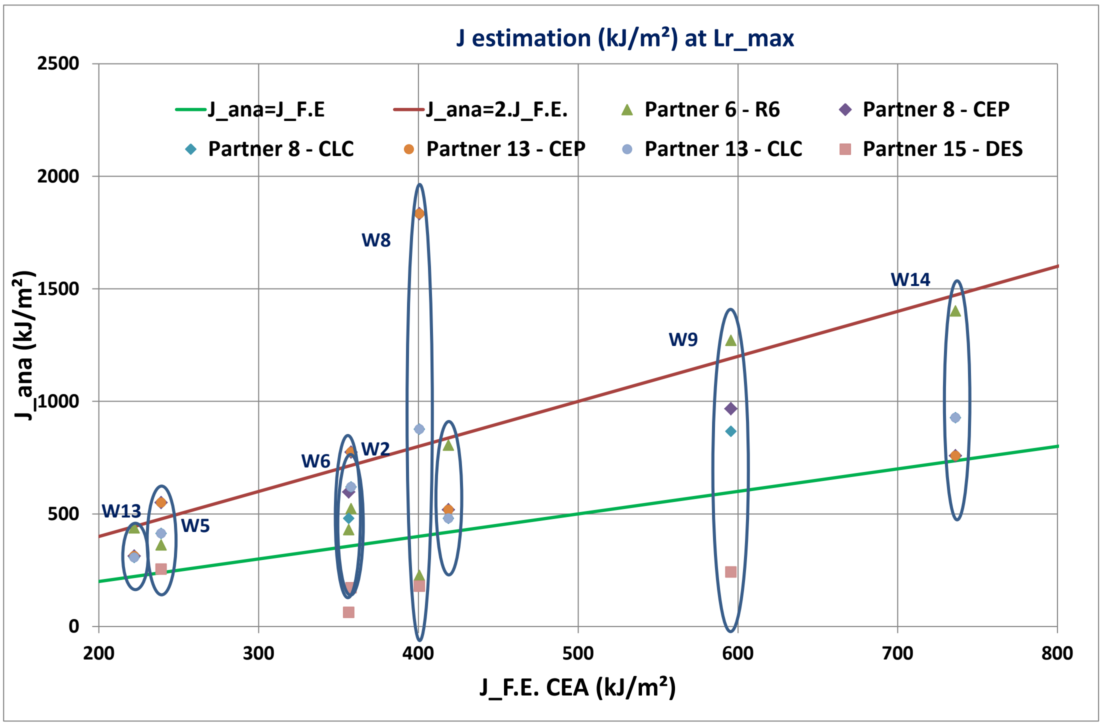

Figure 37: Scatter on J estimation results at maximum level of load for the different configurations investigated in task 6

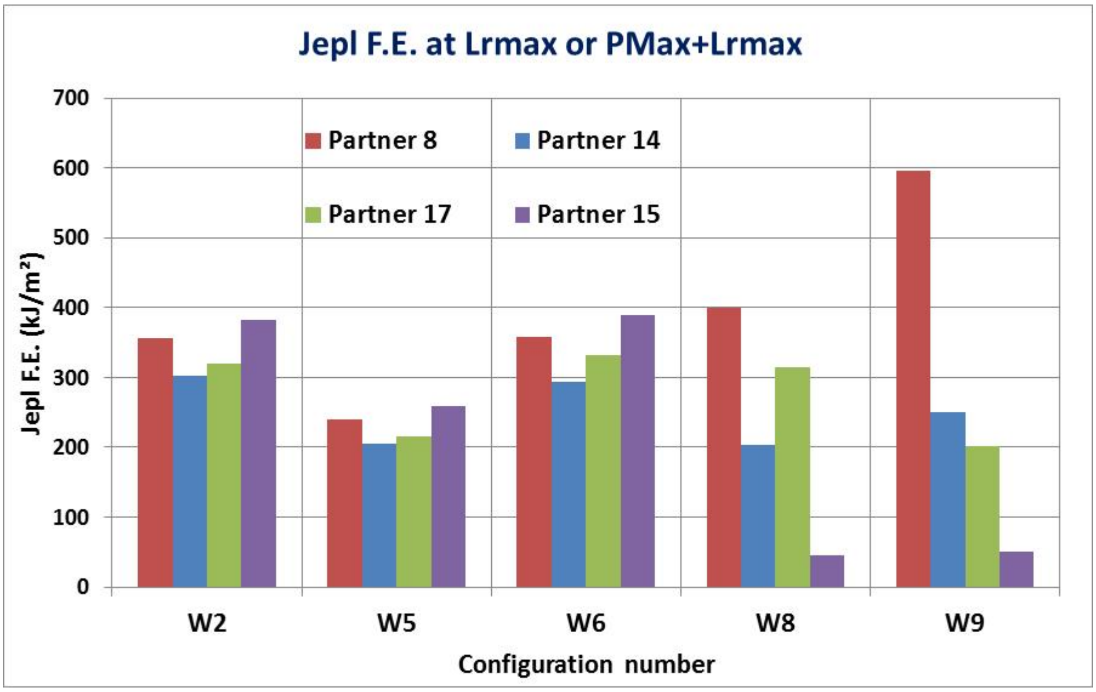

Figure 2. Figure 38: Comparison of J_{epl} values obtained by FE analysis at maximum level of load

Figure 3.

8. TASK7 – DISCUSSION AND CONCLUSIONS

This report presents the work performed in the "BENCH-KJ" benchmark launched in the frame of the OECD NEA CSNI WGIAGE METAL group on fracture mechanic parameters calculation. Twenty-two partners were globally involved, level of contribution depending on the considered technical task keeping in mind that it relies on in-kind participations. Main conclusions are the following:

- **Task 1 – K_I:** considering different codes used, results are globally homogeneous and in good agreement with FE reference solutions but some discrepancy persists, in particular with ASME users.
- **Tasks 2 and 3 – J in cracked pipes:** AFCEN codes users globally provided homogeneous results, and in good agreement with FE solutions whereas much more discrepancy is obtained between R6 users. Thermal load sometimes leads to large over-estimated J value (in particular for BS and R6 rules).
- **Task 4 – J in cracked elbows:** for such complex geometry considering analytical solutions, only AFCEN codes have been used and lead to similar results between partners with some restriction for bending moment.
- **Task 5 – particular cases:** only one analytical contribution has been received for imposed displacement consideration (AFCEN code which gives satisfactory results). In the same way, for embedded cracks, only RCC-MRx has been used and conduct to homogeneous value of K_I.
- **Task 6 – J in weld:** Although the number of requested benchmark evaluations were decreased as the activity progressed, a relatively small number of contributions were received for this technical task. Additionally, this task was the most difficult to evaluate which may explain why several participants performed FE computations in parallel with their code evaluations. The various FE results exhibit differences which would require further investigation to understand. Users of the R6 and AFCEN code provided conservative results, and it should be noted that the R6 contributor considered the effects of residual stresses.

This benchmark appeared to be a complex exercise, even the first step of benchmark definition which needs to be as exhaustive as possible. Participants, international practice and used codes weren't known in advance. Consequently many precisions in the definition of the calculation cases were necessary to clarify the differences in the configurations investigated, especially concerning: real shape of defect, how to apply load/boundary condition, load sign especially in the case of combined loading in complex geometry such as elbows, caps effect, pressure on crack faces and the consideration of residual stresses.

It can be concluded that analytical fracture mechanical methods are able to compute linear-elastic K, but also elastic-plastic J, close to finite element results, if proper formulated. This statement holds even for significant plastic effects and J values well above typical crack initiation thresholds. Analytical methods from various sources are applied from the participants, while many of them are in certain relations, but may differ in details. Besides it must be mentioned that most of these approaches intentionally involves conservative elements with the consequence that, especially at high level of load, large conservatism can be observed.

It has to be noticed that as a consequence of some mistakes done during this benchmark, some improvements of codes as an example RSE-M (AFCEN code) are actually undertaken; most of them simply consists in text reformulation in order to avoid user misunderstanding.

From a certain point of view, it can be understood that there is a real need for codes to be as prescriptive as possible in order to avoid human errors as load considerations (as already said considering pressure on crack places, clear orientation of bending moment, ratio two on imposed displacement…), localisation of defect (different sections may be possible in elbows). The challenge consists in conciliating this requirement of sufficient guidance with an acceptable ease of use.

For this purpose, it can be noticed that some participants made use of an initiative conducted by CEA which developed a freely distributed tool, called MJSAM, which provides all fracture mechanics methods available in RCC-MRx appendix A16 (similar than appendix 5.4 of RSE-M). Other participants relied on implementations in fracture mechanical tools, such as the GRS-code PROST. This kind of software tools radically ease the application of analytical methods available in actual codes and standards, may improve the reliability of the methods and allow deeper understanding on their accuracy. It is recommendable to use such software tools, if available, for avoiding user misunderstandings.

Indeed BENCH-KJ exercise shouldn't be considered as a deep analysis of code accuracy reminding it relies on in kind contribution (contributions and their analysis are in fact time consuming), some approaches were based on "mixed" methods, skill level of participants goes from trainees to fracture mechanics expert, some partners provided updated result others not, and finally some partners regularly undertook FE analysis (rather than analytical methods).

Finally it should be mentioned that KJ benchmark recommends some further developments which may be useful in C&S such as consideration of thermal loads (it seems that R6 workgroup recently performed some improvements on this point) and residual stresses (as an example there's nothing on this point in AFCEN codes).

9. REFERENCES

[1] RSE-M Code, "Rules for In-service Inspection of Nuclear Power Plant Components", 1997 Edition + 1998, 2000 and 2005 addenda, AFCEN, Paris.

[2] RCC-MRx Code, 2010 edition, "Design and Construction Rules for Mechanical Components of FBR Nuclear Islands and high temperature applications" Appendix A16, Tome I, vol. Z, 2010, Paris, AFCEN, Paris.

[3] R6, Assessment of the Integrity of Structures Containing Defects, Revision 4, British Energy Generation, Gloucester, United Kingdom, 2006.

[4] ASME Code, Section XI, Appendices A and C.

[5] API recommended practice 579. First edition, January 2000. American petroleum Institute.

[6] BENCH-KJ, "Benchmark on the analytical evaluation of the fracture mechanic parameters K and J for different components and loads – Rev. 3', 2011, OCDE/IAGE document.

[7] Marie, S. & Faidy, C., "Bench-KJ: Benchmark on analytical calculation of Fracture Mechanics parameters K_I and J for cracked piping components – progress of the work", 2013 PVP conference, Paris (France).

[8] Marie, S., Chapuliot, S., Kayser, Y., Lacire, M.H., Drubay, B. Barthelet, B., Le Delliou, P., Rougier, V., Naudin, C., Gilles, P. and Triay, M., "French RSE-M and RCC-MR code appendixes for flaw analysis: Presentation of the fracture parameters calculation – Part V: Elements of validation", *International Journal of Pressure Vessels and Piping*, 2007, Vol. 84, pp.687-696.

[9] BS 7910: 2005 – "Guide to methods for assessing the acceptability of flaws in metallic structures".

[10] Kayser Y., Marie, S., Chapuliot, S., Le Ledelliou, P., Faidy, C., "Bench-KJ: benchmark on analytical calculation of Fracture Mechanics parameters K_I and J for crack piping components– Final results and conclusion", 2015 SMiRT 23 conference, Manchester.

[11] Marie, S., "BenchKJ : Benchmark on analytical methods for the Fracture Mechanics parameters calculation – 2012 progress report" CEA report DEN/DANS/DM2S/SEMT/LISN/RT/13-038/A.

[12] Marie, S., "BenchKJ: 2013 progress report" CEA report DEN/DANS/DM2S/SEMT/ LISN/RT/14-002/A.

[13] Zahoor, A., "Ductile Fracture Handbook" Vol.1-3, EPRI NP-6301-D, 1989-1991.

[14] M. Busch, M. Petersilge, I. Varfolomeyev: Polynomial Influence Functions for Surface Cracks in Pressure Vessel Components. IWM-Report Z 11/95, October 1995.

[15] Al Laham, S., "Stress Intensity Factor and Limit Load Handbook", EPD/GEN/REP/0316/98, SINTAP/Task 2.6, April 1998.

[16] Schwalbe, K.-H., Kim, Y.-J., Hao, S., Cornec, A., Kocak, M., "EFAM ETM-MM96 – the ETM Method for assessing the significance of crack-like defects in joints with mechanical heterogeneity (strength-mismatch).

[17] Dillstrom P. et al, A Combined Deterministic and Probabilistic Procedure for Safety Assessment of Components with Cracs – Handbook, SSM Research Report 2008:1, Swedish Radiation Safety Authority, 2009 (available on SSM website).

APPENDIX

The appendix was drafted in 2010 to present input and preliminary working plans, as well as schedules for the activity.

BENCH-KJ

Benchmark on the analytical evaluation of the fracture mechanic parameters K and J for different components and loads

Description of all the different cases

Prepared by:

Stephane MARIE
CEA-DEN
Phone: +33 1 69 08 92 57
Fax: +33 1 69 08 87 84
e-mail : stephane.marie@cea.fr

Claude FAIDY
EDF-SEPTEN
Phone: +33 4 7282 7279
Fax: +33 4 7282 7697
e-mail : claude.faidy@edf.fr

Review by :
Stéphane CHAPULIOT - AREVA
Patrick LE DELLIOU - EDF
Yann KAYSER - CEA

2. INTRODUCTION

For many ageing considerations fracture mechanics is needed to evaluate cracked components. The major parameters used are K and J. For that, the different codes (RSE-M appendix 5, RCCMRx appendix A16, R6 rule, ASME B&PV Code Section XI, API, VERLIFE, Russian Code…) propose compendia of stress intensity factors, and for some of them compendia of limit loads for usual situations, in terms of component geometry, type of defect and loading conditions. The benchmark aims to compare these different estimation schemes by comparison to a reference analysis done by Finite Element Method, for representative cases (pipes and elbows, mechanical or/and thermal loadings, different type and size of cracks).

The objective is to have a global comparison of the procedures but also of all independent elements as stress intensity factor or reference stress.

The benchmark will cover simple cases with basic mechanical loads like pressure and bending up to complex load combinations and complex geometries (cylinders and elbows) including cladding or welds. This project is a basic task for analysing damage mechanisms and residual life of components. It's an essential reference task to train new people in the field of damage analysis.

AEN NEA — IAGE Integrity of Components and Structures — OECD

3. Glossary

a	Defect depth
c	Surface half length of the defect
CDSI	Circumferential semi-elliptical internal defect
CDRI	Circumferential rectangular internal defect
CDSE	Circumferential semi-elliptical external defect
CDAI	Circumferential axisymetric internal defect
CDAE	Circumferential axisymetric external defect
$J_{el,A}$	Elastic value of J at the defect deepest point
J_A	Elastic-Plastic value of J at the defect deepest point
$J_{el,C}$	Elastic value of J at the defect surface point
J_C	Elastic-Plastic value of J at the defect surface point
J_s	Analytical value of J
J^{th}	J value related to thermal loading
J^{me}	J value related to mechanical loading
J^{me+th}	J value for combined thermal+mechanical loading
$K_{I,A}$	Elastic stress intensity factor at the defect deepest point
$K_{I,C}$	Elastic stress intensity factor at the defect surface point
k_{th}	Plasticity correction of J_e under thermal loadings
LDII	Longitudinal infinite internal defect
LDIE	Longitudinal infinite external defect
LDSI	Longitudinal semi-elliptical internal defect
LDSE	Longitudinal semi-elliptical external defect
φ_{Jth}	Amplification of the J due to the interaction between mechanical and thermal loadings : $\varphi_{Jth} = \dfrac{\sqrt{J_s^{me+th}} - \sqrt{J_s^{me}}}{\sqrt{J_s^{th}}}$
ε_{ref}	Reference strain
σ_{ref}	Reference stress
ϕ	Weld angle
Hi	Weld root height

All required material properties for the analyses must be provided. It concerns at least :

- the Young modulus E (MPa),
- the Poisson ratio ν,
- the yield stress $\sigma_{y,0.2\%}$ (MPa),
- the thermal expansion coefficient **ALFA (°C^{-1})** if needed,
- the stress-strain curve by points of the material,
- if applicable, the coefficients of the Ramberg-Osgood law : n, σ_0 (MPa) and α

$$\varepsilon = \frac{\sigma}{E} + \alpha \cdot \frac{\sigma_0}{E} \cdot \left(\frac{\sigma}{\sigma_0}\right)^n$$

Additional data can be provided, as for example in the case of thermal loading :

- the volumic weight ρ (kg/m^3),
- the specific heat C_p (J/Kg/°C),
- the thermal conductivity λ (W/M/°C).

4. Reference figures

4.1. cylinder definition

Geometry of the tube

- r_i : internal radius
- r_e : external radius
- D_e : external diameter
- r_m : average radius
- **h** : thickness
- L_{tube} : length

Loads

- **P** : internal pressure
- $\mathbf{M_1}$: torsion moment along the axis 1
- $\mathbf{M_2}$: global bending moment along axis 2
- $\mathbf{N_1}$: axial load (without pressure effect on the end closure)
- ΔT_1 : Linear through-thickness temperature variation
- ΔT_2 : Quadratic through-thickness temperature variation

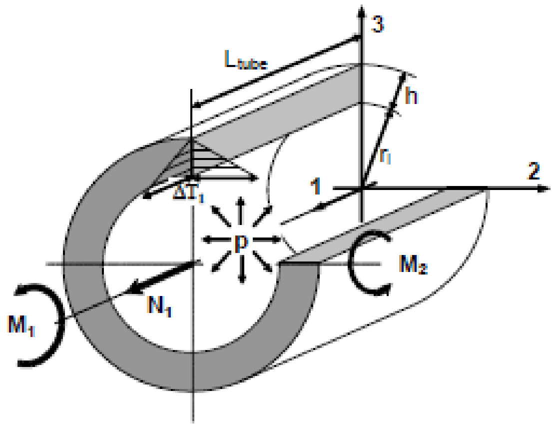

4.2. Surface crack in cylinder

Geometry of the defect CDSI
(Circumferential semi-elliptical internal defect)

- **a** : depth of the defect
- **2c** : length of the defect ($2c = 2\beta.r_i$)
- 2β : angle of the defect (in radians) symmetrical position in relation to the bending plane

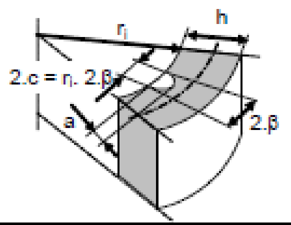

Geometry of the defect CDAI
(Circumferential axisymmetric internal defect)

- **A** : depth of the defect

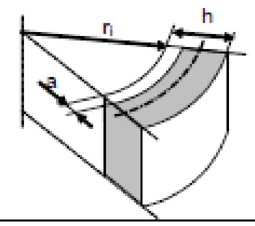

Geometry of the defect LDSI
(Longitudinal semi-elliptical internal defect)

- **a** : depth of the defect
- **2c** : length of the defect

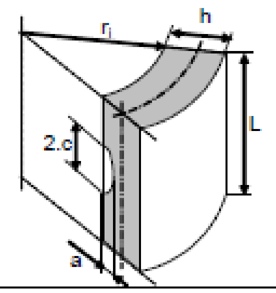

4.3. Through wall crack in cylinder

<table>
<tr>
<td>Geometry of the defect CTR
(Circumferential through wall defect)

Geometry of the defect
2c : length of the defect (2c = 2β.rm)
2β : angle of the defect (in radians), symmetrical position in relation to the bending plane</td>
<td>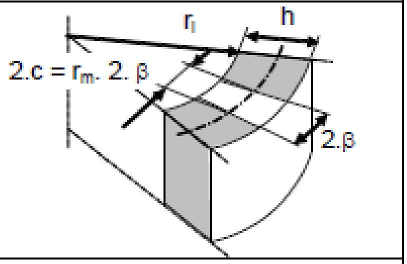
</td>
</tr>
<tr>
<td>Geometry of the defect LTR
(Longitudinal through wall defect)

Geometry of the defect
2c : length of the defect</td>
<td>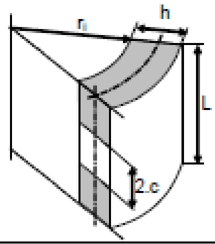
</td>
</tr>
</table>

4.4. Cracks in cladded components

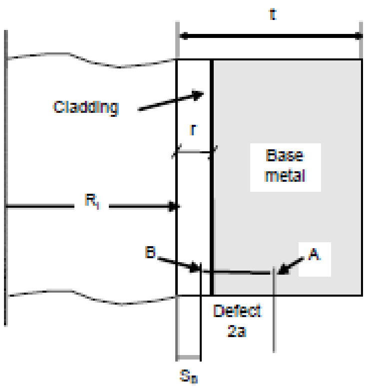

4.5. Embedded cracks

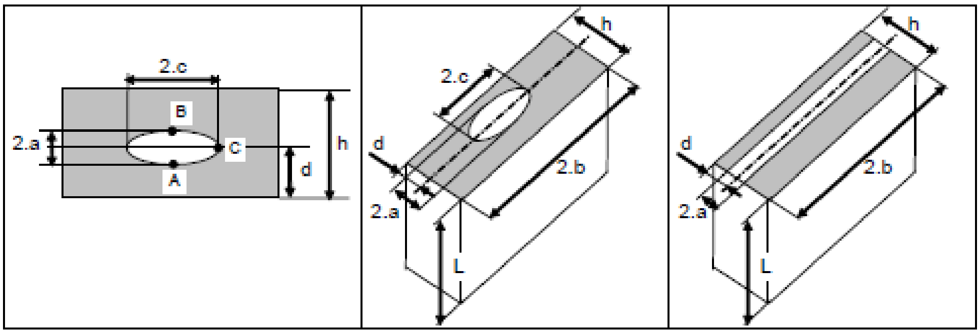

AEN NEA — IAGE Integrity of Components and Structures — OECD

4.6. cracked elbows definition

r_i : internal radius r_e : external radius D_e : external diameter r_m : average radius $r_m = r_e - \frac{h}{2}$ R_c : bend radius	φ : azimut in the cross section (radian) **h** : thickness If there is extra thickness on the inside surface: h(φ) : thickness as a function of azimuth $h = \frac{1}{2\pi}\cdot\int_0^{2\pi} h(\varphi)\cdot d\varphi$: average thickness	$Z = \pi\cdot r_m{}^2 .h$ $\quad\lambda = \frac{h\cdot R_c}{r_m^2}$ $X = \frac{r_m}{h}$ $\quad L_a = \sqrt{\frac{r_m^3}{h}}$
ψ_c : elbow bend radius (in radians) = angle between the entrance section and the exit section of the elbow 30° elbow : $\psi_c = \pi/6$ 45° elbow : $\psi_c = \pi/4$ 90° elbow : $\psi_c = \pi/2$ 180° elbow : $\psi_c = \pi$	ψ : angle in radians between the entrance section and the considered section ψ=0 : elbow entrance section $\psi=\psi_c/2$: elbow median section $\psi=\psi_c$: elbow exit section	**P** : internal pressure
Moments in the entrance section M_1^0 : torsion moment M_2^0 : in plane bending moment M_3^0 : out plane bending moment	**Moments in a given section** $M_1 = M_1^0\cdot\cos\psi - M_3^0\cdot\sin\psi$ $M_2 = M_2^0$ $M_3 = M_1^0\cdot\sin\psi + M_3^0\cdot\cos\psi$	**Moments in the mid section** $M_1\left(\frac{\psi_c}{2}\right) = M_1^0\cdot\cos\left(\frac{\psi_c}{2}\right) - M_3^0\cdot\sin\left(\frac{\psi_c}{2}\right)$ $M_2\left(\frac{\psi_c}{2}\right) = M_2^0$ $M_3\left(\frac{\psi_c}{2}\right) = M_1^0\cdot\sin\left(\frac{\psi_c}{2}\right) + M_3^0\cdot\cos\left(\frac{\psi_c}{2}\right)$

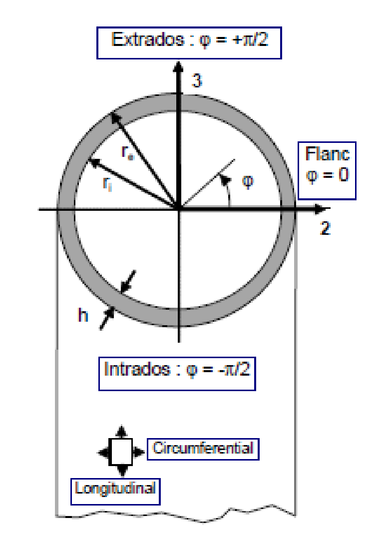

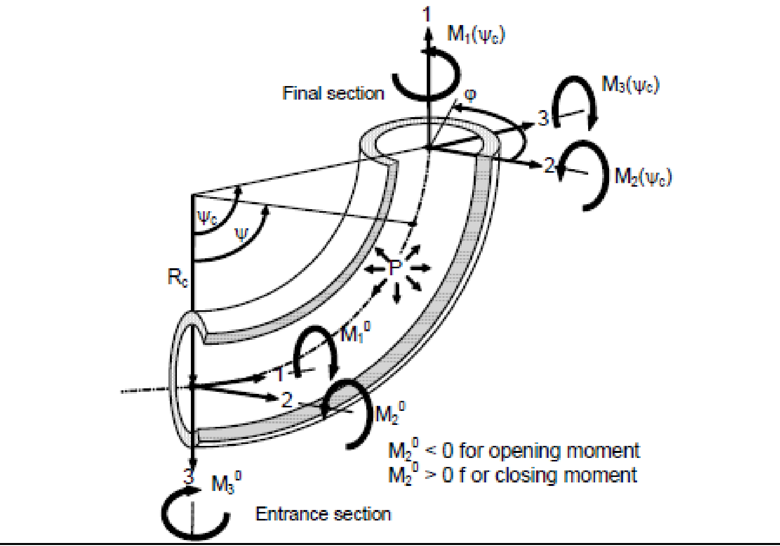

Geometry of the defect CDSI (Circumferential semi-elliptical internal defect)		
Extrados	Crown	Intrados
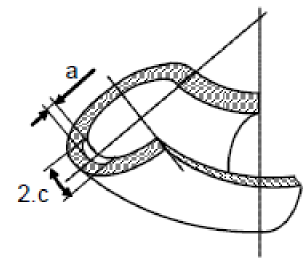	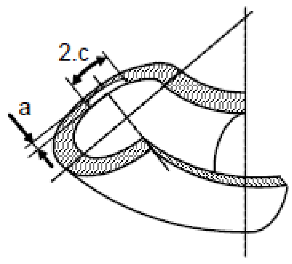	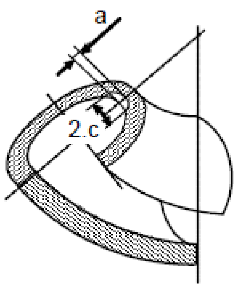

Geometry of the defect LDSI (Circumferential semi-elliptical internal defect)	
Intrados	Extrados
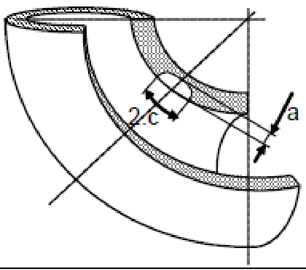	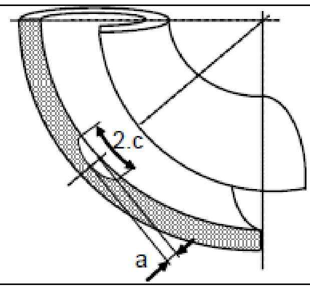

5. Task 1 : Elastic K evaluation

This first task is to compare the application of the different procedures for the stress intensity factor in two situations:

- a cracked pipe under mechanical loading
- a cracked plate under thermal loading (exponential distribution of the elastic nominal stress)

5.1. Circumferential surface crack in cylinder

It is propose to compare the stress intensity factor solutions for the three following geometries:

GEOMETRY						
Case #	Geometry #	Defect	a/h	c/a	h (mm)	De (mm)
K1	PIPE 1	CDAI – circumferetial internal axysimetric	0.1 – 0.25 – 0.5 – 0.75	-	60	660
K2	PIPE 2	CDAE – circumferetial external axysimetric	0.1 – 0.25 – 0.5 – 0.75	-	60	660
K3	PIPE 3	CDSI – circumferetial internal semi-elliptical	0.1 – 0.25 – 0.5 – 0.75	3	60	660

The material data to use are provided in following table :

E (MPa)	ν
177000	0.3

For these geometries, the two following loading conditions are considered:

Loading codition #	P (MPa)	M1 (N.mm)	M2 (N.mm)
1	25	-	3.50E+09
2	-	1.70E+09	5.20E+09

Appendix 1.1 provides the result table for this application.

5.2. Longitudinal surface crack in cylinder

It is propose to compare the stress intensity factor solutions for the two following geometries:

GEOMETRY						
Case #	Geometry #	Defect	a/h	c/a	h (mm)	De (mm)
K4	PIPE 1	LDII – longitudinal internal infinite	0.1 – 0.25 – 0.5 – 0.75	-	60	660
K5	PIPE 2	LDSI – longitudinal internal semi-elliptical	0.1 – 0.25 – 0.5 – 0.75	3	60	660

The material data to use are provided in following table :

E (MPa)	v
177000	0.3

For these geometries, the two following loading conditions are considered:

Loading condition #	P (MPa)	M1 (N.mm)	M2 (N.mm)
1	50	-	-
2	50	-	6.0E+09

Appendix 1.1 provide the result table for this application.

5.3. Plate under thermal loading

The geometry is a plate with an infinite surface crack characterized by the normalized depth a/h. The plate thickness is 10 mm. The plate is submitted to a stress through thickness distribution relevant of a thermal load. This distribution is provided in the following table :

Relative position in the thickness	Stress
0	151.245
0.1	99.666
0.2	52.624
0.3	19.844
0.4	1.453
0.5	-6.304
0.6	-7.746
0.7	-6.276
0.8	-4.026
0.9	-2.059
1	-0.726

The material data to use are provided in following table :

E (MPa)	v
177000	0.3

It is asked to calculate the elastic stress intensity factor for the defect size a/h = 0.1, 0.2, 0.3, 0.4, 0.5, 0.6, 0.7, 0.8. Appendix 1.2 provides the result table for this application.

6. Task 2: Plastic J evaluation for surface crack in cylinders

It is proposed to compare the different procedures for the analytical J calculation for pipes with a surface crack

- the first list concerns pure mechanical loadings for pipes with a circumferential defect
- the second list concerns pure mechanical loadings for pipes with an axial defect
- the third list concerns pure thermal loadings for pipes with a circumferential or an axial defect
- the last list concerns combined mechanical & thermal loadings for pipes with a circumferential or an axial defect

For each case, the geometry and the material are specified. A loading variation is proposed. The extremes of this variation are specified. For the analyses, each phase of the mechanical loading variation will be decomposed into 5 steps. When the case concerns are combined mechanical & thermal loading condition, the initial values (elastic and elastic-plastic) for the initial mechanical loading have to be calculated.

Specific answer sheets are provided in Appendix 2. It is asked to calculate the elastic and elastic-plastic value of J. If possible, the reference stress can be also introduced in the result tables.

6.1. Material properties

Four materials are considered for the following analyses.

6.1.1. material n5

E (MPa)	ν	$\sigma_{y,0.2\%}$ (MPa)	ALFA (°C^{-1})	n	σ_0 (MPa)	α
177000	0.3	119.60	1.77E-05	5	120	3

SIG (MPa)	EPS (%)
0	0.00E+00
60	3.39E-02
70	5.33E-02
80	7.20E-02
90	9.91E-02
100	1.38E-01
110	1.94E-01
120	2.71E-01
130	3.77E-01
140	5.19E-01
150	7.05E-01
160	9.47E-01
170	1.26E+00
180	1.65E+00
190	2.13E+00
200	2.73E+00

SIG (MPa)	EPS (%)
210	3.46E+00
220	4.34E+00
230	5.39E+00
240	6.64E+00
250	8.12E+00
260	9.86E+00
270	1.19E+01
280	1.42E+01
290	1.69E+01
300	2.00E+01
310	2.36E+01
320	2.76E+01
330	3.22E+01
340	3.73E+01
350	4.31E+01

6.1.2. material n6

E (MPa)	ν	$\sigma_{y,0.2\%}$ (MPa)	ALFA (°C^{-1})	n	σ_0 (MPa)	α
174700	0.3	185.1	1.81E-05	6	163	1.00E+00

SIG (MPa)	EPS (%)
0	0.000E+00
10	5.724E-03
20	1.145E-02
30	1.718E-02
40	2.292E-02
50	2.870E-02
60	3.458E-02
70	4.065E-02
80	4.710E-02
90	5.416E-02
100	6.222E-02
110	7.178E-02
120	8.354E-02
130	9.843E-02
140	1.176E-01
150	1.425E-01
160	1.750E-01
170	2.174E-01
180	2.722E-01
190	3.428E-01
200	4.329E-01

SIG (MPa)	EPS (%)
210	5.469E-01
220	6.900E-01
230	8.681E-01
240	1.088E+00
250	1.358E+00
260	1.686E+00
270	2.082E+00
280	2.558E+00
290	3.125E+00
300	3.798E+00
310	4.593E+00
320	5.525E+00
330	6.614E+00
340	7.880E+00
350	9.345E+00
360	1.103E+01
370	1.298E+01
380	1.520E+01
390	1.773E+01
400	2.061E+01
500	4.938E+01

6.1.3. material n8

E (MPa)	ν	$\sigma_{y,0.2\%}$ (MPa)	ALFA (°C^{-1})	n	σ_0 (MPa)	α
177000	0.3	119.7		8	120	3

SIG (MPa)	EPS (%)
0	0.00E+00
60	3.390E-02
70	4.227E-02
80	5.313E-02
90	7.121E-02
100	1.038E-01
110	1.635E-01
120	2.712E-01
130	4.593E-01
140	7.772E-01
150	1.297E+00
160	2.122E+00
170	3.396E+00
180	5.314E+00
190	8.141E+00
200	1.222E+01

SIG (MPa)	EPS (%)
210	1.801E+01
220	2.608E+01
230	3.717E+01
240	5.220E+01
250	7.232E+01
260	9.893E+01
270	1.337E+02
280	1.789E+02
290	2.368E+02
300	3.105E+02
310	4.036E+02
320	5.203E+02
330	6.654E+02
340	8.449E+02
350	1.065E+03

6.1.4. material 316

E (MPa)	ν	$\sigma_{y,0.2\%}$ (MPa)	ALFA (°C^{-1})	n	σ_0 (MPa)	α
176500	0.3	133	1.77E-05	-	-	-

SIG (MPa)	EPS (%)
0.0	0.000
111.0	0.063
117.0	0.101
124.0	0.170
133.0	0.275
145.0	0.482
154.0	0.687
159.0	0.890
163.0	1.092
172.0	1.597
179.0	2.101

SIG (MPa)	EPS (%)
193.0	3.000
206.0	4.000
265.0	8.000
348.0	14.00
420.0	20.00
500.0	28.11
600.0	39.98
700.0	53.85
900.0	88.71
1000.0	107.3

AEN NEA — IAGE Integrity of Components and Structures — OECD

6.2. Circumferential defects

Case #	Geometry		Material	Loading	
Pipe C1	CDAI De (mm) h (mm) a (mm)	- 660 60 7.5	n5	$M_{2,max}$ = 5,22E9 N.mm	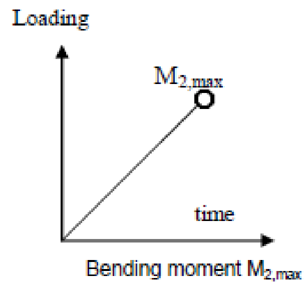
Pipe C2	CDAI De (mm) h (mm) a (mm)	- 660 60 15	n5	$M_{2,max}$ = 5,22E9 N.mm	
Pipe C3	CDSI De (mm) h (mm) a (mm) c (mm)	- 660 60 15 45	n5	$M_{2,max}$ = 5,22E9 N.mm	
Pipe C4	CDSI De (mm) h (mm) a (mm) c (mm)	- 660 60 15 45	n5	$M_{1,max}$ = 4,70E9 N.mm	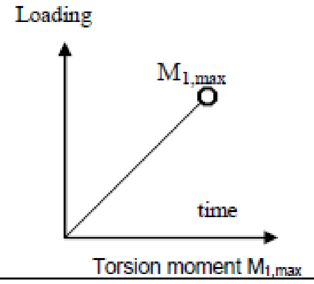
Pipe C5	CDSE De (mm) h (mm) a (mm) c (mm)	- 660 60 15 45	n8	$M_{2,max}$ = 5,22E9 N.mm	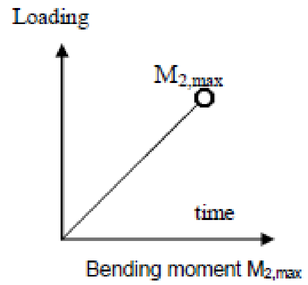
Pipe C6	CDRI De (mm) h (mm) a (mm) c (mm)	- 660 60 7.5 212	n5	$M_{2,max}$ = 5,22E9 N.mm	
Pipe C7	CDRI De (mm) h (mm) a (mm) c (mm)	- 660 60 15 212	n5	$M_{2,max}$ = 5,22E9 N.mm	
Pipe C8	CDAI De (mm) h (mm) a (mm)	- 660 60 7.5	n5	P_{max} = 21.2 Mpa $M_{2,max}$ = 5,22E9 N.mm	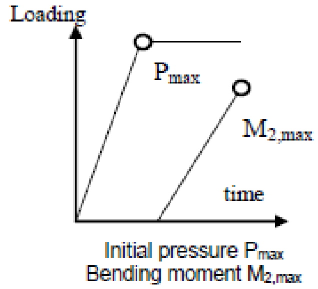
Pipe C9	CDSI De (mm) h (mm) a (mm) c (mm)	- 660 60 15 45	n5	P_{max} = 12 MPa $M_{2,max}$ = 5,22E9 N.mm	
Pipe C10	CDSI De (mm) h (mm) a (mm) c (mm)	- 840 40 10 60	n5	P_{max} = 10,6 MPa $M_{2,max}$ = 6,15E9 N.mm	
Pipe C11	CDSE De (mm) h (mm) a (mm) c (mm)	- 660 60 15 45	n8	P_{max} = 36 MPa $M_{2,max}$ = 4,93E9 N.mm	

AEN NEA — IAGE Integrity of Components and Structures — OECD

6.2. Circumferential defects

Case #	Geometry		Material	Loading	
Pipe C1	CDAI D_e (mm) h (mm) a (mm)	- 660 60 7.5	n5	$M_{2,max}$ = 5,22E9 N.mm	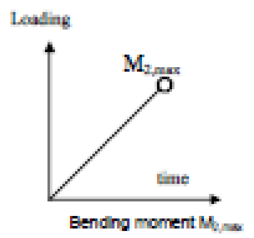
Pipe C2	CDAI D_e (mm) h (mm) a (mm)	- 660 60 15	n5	$M_{2,max}$ = 5,22E9 N.mm	
Pipe C3	CDSI D_e (mm) h (mm) a (mm) c (mm)	- 660 60 15 45	n5	$M_{2,max}$ = 5,22E9 N.mm	
Pipe C4	CDSI D_e (mm) h (mm) a (mm) c (mm)	- 660 60 15 45	n5	$M_{1,max}$ = 4,70E9 N.mm	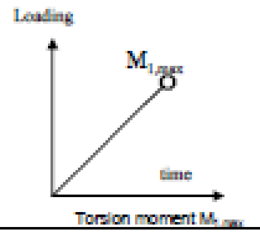
Pipe C5	CDSE D_e (mm) h (mm) a (mm) c (mm)	- 660 60 15 45	n8	$M_{2,max}$ = 5,22E9 N.mm	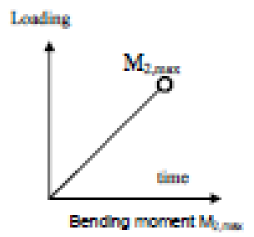
Pipe C6	CDRI D_e (mm) h (mm) a (mm) c (mm)	- 660 60 7.5 212	n5	$M_{2,max}$ = 5,22E9 N.mm	
Pipe C7	CDRI D_e (mm) h (mm) a (mm) c (mm)	- 660 60 15 212	n5	$M_{2,max}$ = 5,22E9 N.mm	
Pipe C8	CDAI D_e (mm) h (mm) a (mm)	- 660 60 7.5	n5	P_{max} = 21.2 Mpa $M_{2,max}$ = 5,22E9 N.mm	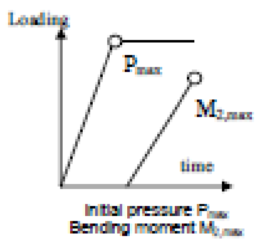
Pipe C9	CDSI D_e (mm) h (mm) a (mm) c (mm)	- 660 60 15 45	n5	P_{max} = 12 MPa $M_{2,max}$ = 5,22E9 N.mm	
Pipe C10	CDSI D_e (mm) h (mm) a (mm) c (mm)	- 840 40 10 60	n5	P_{max} = 10,6 MPa $M_{2,max}$ = 6,15E9 N.mm	
Pipe C11	CDSE D_e (mm) h (mm) a (mm) c (mm)	- 660 60 15 45	n8	P_{max} = 36 MPa $M_{2,max}$ = 4,93E9 N.mm	

- 16 -

AEN NEA — IAGE Integrity of Components and Structures — OECD

6.3. Longitudinal defects

Case #	Geometry		Material	Loading	
Pipe L1	LDSI D_e (mm) h (mm) a (mm) c (mm)	- 660 60 15 45	n6	$M_{1,max}$ =7,23E9 N.mm	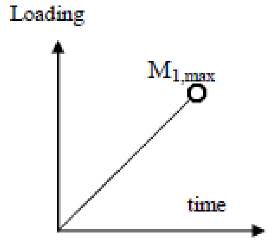 Torsion moment $M_{1,max}$
Pipe L2	LDII D_e (mm) h (mm) a (mm)	- 660 60 7.5	n6	P_{max} = 41 MPa $M_{2,max}$ = 5,22E9 N.mm	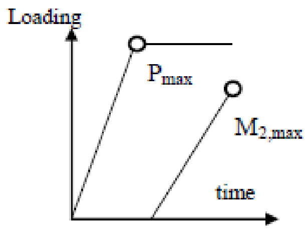 Initial pressure P_{max} Bending moment $M_{2,ma}$
Pipe L3	LDII D_e (mm) h (mm) a (mm)	- 660 60 7.5	n6	P_{max} = 20,55 MPa $M_{2,max}$ = 5,22E9 N.mm	
Pipe L4	LDIE D_e (mm) h (mm) a (mm)	- 660 60 7.5	n6	P_{max} = 20,55 MPa $M_{2,max}$ = 5,22E9 N.mm	
Pipe L5	LDSI D_e (mm) h (mm) a (mm) c (mm)	- 660 60 7.5 22.5	n6	P_{max} = 20,55 MPa $M_{2,max}$ = 5,22E9 N.mm	
Pipe L6	LDSI D_e (mm) h (mm) a (mm) c (mm)	- 660 60 15 45	n6	P_{max} = 20,5 MPa $M_{2,max}$ = 5,22E9 N.mm	
Pipe L7	LDSI D_e (mm) h (mm) a (mm) c (mm)	- 660 60 15 45	n6	P_{max} = 20,55 MPa $M_{1,max}$ = 7,23E9 N.mm	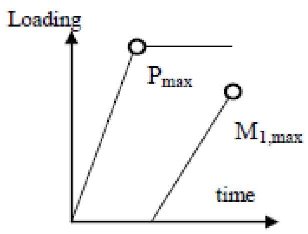 Initial pressure P_{max} Torsion moment $M_{1,max}$
Pipe L8	LDSE D_e (mm) h (mm) a (mm) c (mm)	- 660 60 15 45	n6	P_{max} = 20,5 MPa $M_{2,max}$ = 5,22E9 N.mm	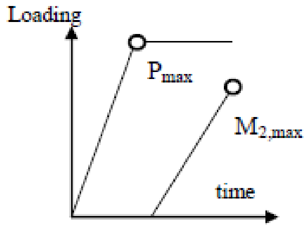 Initial pressure P_{max} Bending moment $M_{2,max}$
Pipe L9	LDSE D_e (mm) h (mm) a (mm) c (mm)	- 660 60 7.5 22.5	n6	P_{max} = 20,5 MPa $M_{2,max}$ = 5,22E9 N.mm	

6.4. Elementary thermal loads

Thermal loading under consideration correspond to a through thickness temperature variation. Two components are considered: a linear variation ΔT_1 and a quadratic variation ΔT_2. The complete temperature variation is then given by :

$$T(\varsigma) = -6 \cdot \Delta T_2 \cdot \varsigma^2 + \Delta T_1 \cdot \varsigma + \frac{\Delta T_2}{2}$$

where ζ is the normalized through-thickness position ($-0.5 < \zeta < 0.5$).

Case #	Geometry		Material	Loading
Pipe L10	LDII D_e (mm) h (mm) a (mm)	- 660 60 2	n6	$\Delta T_{1,max}$ = 213 °C $\Delta T_{2,max} / \Delta T_{1,max}$ = 0.1778
Pipe L11	LDII D_e (mm) h (mm) a (mm)	- 660 60 7.5	n6	$\Delta T_{1,max}$ = 194 °C $\Delta T_{2,max} / \Delta T_{1,max}$ = 0.1778
Pipe L12	LDII D_e (mm) h (mm) a (mm)	- 660 60 15	n6	$\Delta T_{1,max}$ = 245 °C $\Delta T_{2,max} / \Delta T_{1,max}$ = 0.1778
Pipe L13	LDII D_e (mm) h (mm) a (mm)	- 660 60 30	n6	$\Delta T_{1,max}$ = 394 °C $\Delta T_{2,max} / \Delta T_{1,max}$ = 0.1778
Pipe L14	LDSI D_e (mm) h (mm) a (mm) c (mm)	- 660 60 15 15	n6	$\Delta T_{1,max}$ = 416 °C $\Delta T_{2,max} / \Delta T_{1,max}$ = 0.172
Pipe L15	LDSI D_e (mm) h (mm) a (mm) c (mm)	- 660 60 20 20	n6	$\Delta T_{1,max}$ = 341 °C $\Delta T_{2,max} / \Delta T_{1,max}$ = 0.172
Pipe L16	LDSI D_e (mm) h (mm) a (mm) c (mm)	- 660 60 20 60	n6	$\Delta T_{1,max}$ = 338 °C $\Delta T_{2,max} / \Delta T_{1,max}$ = 0.1778

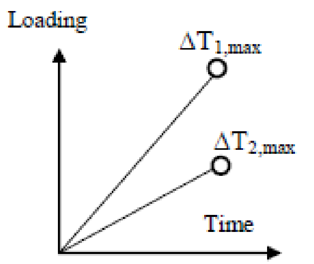

Trough thickness temperature linear variation $\Delta T_{1,max}$

$\Delta T_{2,max} / \Delta T_{1,max}$ = constant

AEN NEA   IAGE Integrity of Components and Structures   OECD

Case #	Geometry		Material	Loading	
Pipe C12	CDAI D_e (mm) h (mm) a (mm)	- 1320 60 1.5	316	$\Delta T_{1,max}$ = 357.6 °C	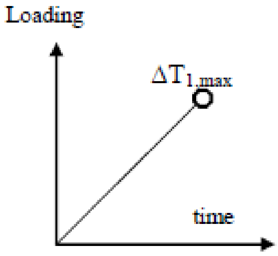 Trough thickness temperature linear variation $\Delta T_{1,max}$
Pipe C13	CDAI D_e (mm) h (mm) a (mm)	- 1320 60 12	316	$\Delta T_{1,max}$ = 357.6°C	
Pipe C14	CDAI D_e (mm) h (mm) a (mm)	- 1320 60 24	316	$\Delta T_{1,max}$ = 357.6°C	
Pipe C15	CDAI D_e (mm) h (mm) a (mm)	- 1320 60 30	316	$\Delta T_{1,max}$ = 357.6°C	
Pipe C16	CDAI D_e (mm) h (mm) a (mm)	- 1320 60 36	316	$\Delta T_{1,max}$ = 357.6°C	
Pipe C17	CDAI D_e (mm) h (mm) a (mm)	- 660 60 2	n6	$\Delta T_{1,max}$ = 247 °C $\Delta T_{2,max}$ / $\Delta T_{1,max}$ = 0.1778	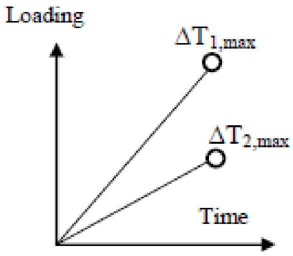 Trough thickness temperature linear variation $\Delta T_{1,max}$ $\Delta T_{2,max}$ / $\Delta T_{1,max}$ = constant
Pipe C18	CDAI D_e (mm) h (mm) a (mm)	- 660 60 3.75	n6	$\Delta T_{1,max}$ = 251 °C $\Delta T_{2,max}$ / $\Delta T_{1,max}$ = 0.1778	
Pipe C19	CDAI D_e (mm) h (mm) a (mm)	- 660 60 7.5	n6	$\Delta T_{1,max}$ = 266.5 °C $\Delta T_{2,max}$ / $\Delta T_{1,max}$ = 0.1778	
Pipe C20	CDAI D_e (mm) h (mm) a (mm)	- 660 60 15	n6	$\Delta T_{1,max}$ = 357 °C $\Delta T_{2,max}$ / $\Delta T_{1,max}$ = 0.1778	
Pipe C21	CDAI D_e (mm) h (mm) a (mm)	- 660 60 30	n6	$\Delta T_{1,max}$ = 459 °C $\Delta T_{2,max}$ / $\Delta T_{1,max}$ = 0.1778	
Pipe C22	CDSI D_e (mm) h (mm) a (mm) c (mm)	- 660 60 7.5 22.5	n6	$\Delta T_{1,max}$ = 266.5 °C $\Delta T_{2,max}$ / $\Delta T_{1,max}$ = 0.1778	
Pipe C23	CDSI D_e (mm) h (mm) a (mm) c (mm)	- 660 60 15 15	n6	$\Delta T_{1,max}$ = 357 °C $\Delta T_{2,max}$ / $\Delta T_{1,max}$ = 0.1778	
Pipe C24	CDSI D_e (mm) h (mm) a (mm) c (mm)	- 660 60 15 45	n6	$\Delta T_{1,max}$ = 357 °C $\Delta T_{2,max}$ / $\Delta T_{1,max}$ = 0.1778	
Pipe C25	CDSI D_e (mm) h (mm) a (mm) c (mm)	- 660 60 30 30	n6	$\Delta T_{1,max}$ = 459 °C $\Delta T_{2,max}$ / $\Delta T_{1,max}$ = 0.1778	

6.5. Mechanical & thermal Load combinations

<table>
<tr><th>Case #</th><th colspan="2">Geometry</th><th>Material</th><th colspan="2">Loading</th></tr>
<tr><td>Pipe C26</td><td>CDAI
D_e (mm)
h (mm)
a (mm)</td><td>-
660
60
15</td><td>316</td><td>$\Delta T_{1,max}$ = 180°C
P_{max} = 29.56 MPa</td><td rowspan="2">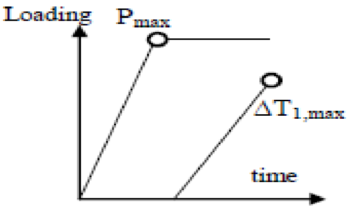

Trough thickness temperature linear variation $\Delta T_{1,max}$ = 180°C
Initial pressure P_{max} = 29.56 MPa</td></tr>
<tr><td>Pipe C27</td><td>CDAI
D_e (mm)
h (mm)
a (mm)</td><td>-
1260
60
15</td><td>316</td><td>$\Delta T_{1,max}$ = 180°C
P_{max} = 14 MPa</td></tr>
<tr><td>Pipe C28</td><td>CDAI
D_e (mm)
h (mm)
a (mm)</td><td>-
660
60
15</td><td>316</td><td>$\Delta T_{1,max}$ = 178.8 °C
P_{max} = 11.82 MPa
$N_{1,max}$ = 1.53E7 N</td><td>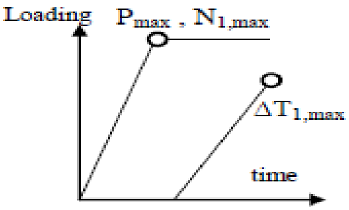

Trough thickness temperature linear variation $\Delta T_{1,max}$
Initial pressure P_{max}
Initial Axial load $N_{1,max}$</td></tr>
<tr><td>Pipe C29</td><td>CDAI
D_e (mm)
h (mm)
a (mm)</td><td>-
660
60
15</td><td>n6</td><td>$\Delta T_{1,max}$ = 357.4 °C
$\Delta T_{2,max}$ / $\Delta T_{1,max}$ = 0.1778
P_{max} = 32 MPa</td><td>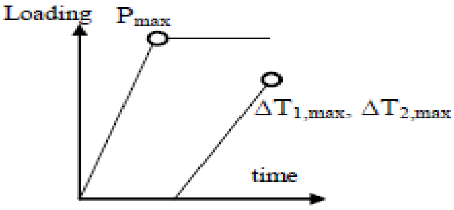

Trough thickness temperature linear variation $\Delta T_{1,max}$
$\Delta T_{2,max}$ / $\Delta T_{1,max}$ = constant
Initial pressure P_{max}</td></tr>
<tr><td>Pipe C30</td><td>CDAI
D_e (mm)
h (mm)
a (mm)</td><td>-
660
60
15</td><td>n6</td><td>$\Delta T_{1,max}$ = 357.4 °C
$\Delta T_{2,max}$ / $\Delta T_{1,max}$ = 0.1778
P_{max} = 19.1 MPa
$N_{1,max}$ = 1.55E7 N</td><td rowspan="2">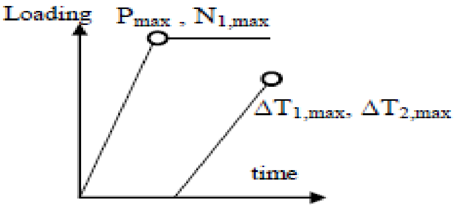

Trough thickness temperature linear variation $\Delta T_{1,max}$
$\Delta T_{2,max}$ / $\Delta T_{1,max}$ = constant
Initial pressure P_{max}
Initial Axial load $N_{1,max}$</td></tr>
<tr><td>Pipe C31</td><td>CDAI
D_e (mm)
h (mm)
a (mm)</td><td>-
660
60
7.5</td><td>n6</td><td>$\Delta T_{1,max}$ = 266.5 °C
$\Delta T_{2,max}$ / $\Delta T_{1,max}$ = 0.1778
I P_{max} = 22.5 MPa
$N_{1,max}$ = 1.01E7 N</td></tr>
</table>

AEN NEA IAGE Integrity of Components and Structures OECD

Case #	Geometry		Material	Loading	
Pipe L18	LDII D_e (mm) h (mm) a (mm)	- 660 60 7.5	n6	$\Delta T_{1,max}$ = 266.5 °C $\Delta T_{2,max}$ / $\Delta T_{1,max}$ = 0.1778 P_{max} = 9.35 MPa	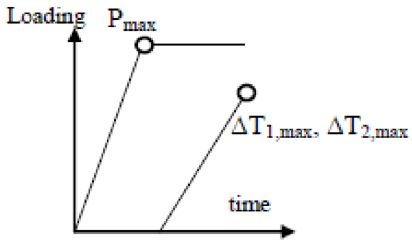 Trough thickness temperature linear variation $\Delta T_{1,max}$ $\Delta T_{2,max}$ / $\Delta T_{1,max}$ = constant Initial pressure P_{max}
Pipe L19	LDII D_e (mm) h (mm) a (mm)	- 660 60 7.5	n6	$\Delta T_{1,max}$ = 266.5 °C $\Delta T_{2,max}$ / $\Delta T_{1,max}$ = 0.1778 P_{max} = 18.7 MPa	
Pipe L20	LDII D_e (mm) h (mm) a (mm)	- 660 60 7.5	n6	$\Delta T_{1,max}$ = 266.5 °C $\Delta T_{2,max}$ / $\Delta T_{1,max}$ = 0.1778 P_{max} = 28.04 MPa	
Pipe L21	LDSI D_e (mm) h (mm) a (mm) c (mm)	- 660 60 15 45	n6	$\Delta T_{1,max}$ = 357.4 °C $\Delta T_{2,max}$ / $\Delta T_{1,max}$ = 0.1778 P_{max} = 28.83 MPa	
Pipe L22	LDSI D_e (mm) h (mm) a (mm) c (mm)	- 660 60 15 45	n6	$\Delta T_{1,max}$ = 357.4 °C $\Delta T_{2,max}$ / $\Delta T_{1,max}$ = 0.1778 $M_{2,max}$ = 2.7e9 N.mm	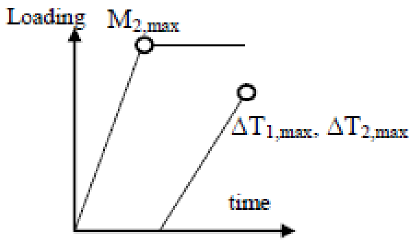 Trough thickness temperature linear variation $\Delta T_{1,max}$ $\Delta T_{2,max}$ / $\Delta T_{1,max}$ = constant Initial bending moment $M_{2,max}$

7. Task 3: Plastic J for through wall cracks in cylinders

It is proposed to compare the different procedures for the analytical J calculation for pipes with a through wall crack under mechanical loading.

For each case, the geometry and the material are specified. A loading variation is proposed. The extremes of this variation are specified. For the analyses, each phase of the mechanical loading variation will be decomposed into 5 steps.

Specific answer sheets are provided in Appendix 2. It is asked to calculate the elastic and elastic-plastic value of J. If possible, the reference stress and the defect opening displacement can be also introduced in the result tables.

7.1. Material properties

one material is considered for the following analyses.

7.1.1. material n7

E (MPa)	ν	$\sigma_{y,0.2\%}$ (MPa)	ALFA (°C^{-1})	n	σ_0 (MPa)	α
200000	0.3	152.6	-	7	130	1

SIG (MPa)	EPS (%)
0.00	0.00
40.95	0.02
42.19	0.02
54.99	0.03
63.83	0.03
70.93	0.04
77.09	0.04
82.67	0.04
87.87	0.05
92.84	0.05
97.66	0.06
102.41	0.06
107.13	0.07
111.87	0.08
116.64	0.09
121.49	0.10
126.43	0.12
131.49	0.14
136.67	0.16
141.99	0.19
147.47	0.23
153.13	0.28
158.96	0.35
164.99	0.43
171.23	0.53

SIG (MPa)	EPS (%)
177.68	0.67
184.36	0.84
191.27	1.07
198.44	1.35
205.86	1.73
213.55	2.20
221.53	2.82
229.79	3.62
238.36	4.65
247.25	5.97
256.46	7.69
266.02	9.90
275.93	12.75
286.20	16.44
296.86	21.19
307.91	27.34
319.38	35.27
331.27	45.51
343.60	58.74
356.39	75.82
369.65	97.88
383.41	126.36
397.68	163.15
412.48	210.66

AEN NEA | IAGE Integrity of Components and Structures | OECD

7.2. Circumferential cracks

Case #	Geometry		Material	Loading	
Pipe CTR1	CTR D_e (mm) h (mm) 2c (mm)	- 660 60 235.6	n7	$N_{1,max}$ = 1,5E7 N	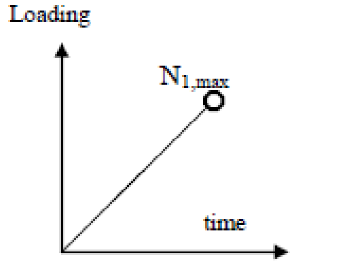 Axial load $N_{1,max}$
Pipe CTR2	CTR D_e (mm) h (mm) 2c (mm)	- 660 60 235.6	n7	$M_{2,max}$ = 2,8E9 N.mm	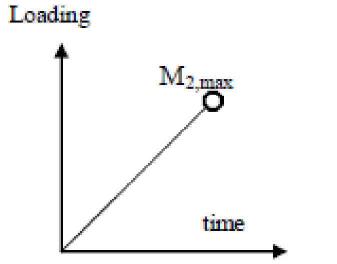 Bending moment $M_{2,max}$
Pipe CTR3	CTR D_e (mm) h (mm) 2c (mm)	- 660 60 117,8	n7	$M_{2,max}$ = 3,5E9 N.mm	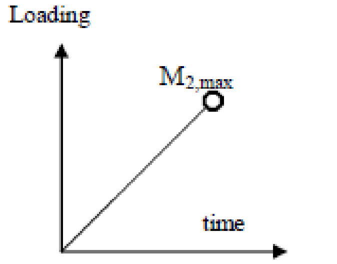 Bending moment $M_{2,max}$
Pipe CTR4	CTR D_e (mm) h (mm) 2c (mm)	- 660 60 235.6	n7	$N_{1,max}$ = 4,9E6 N $M_{2,max}$ = 2,5E9 N.mm	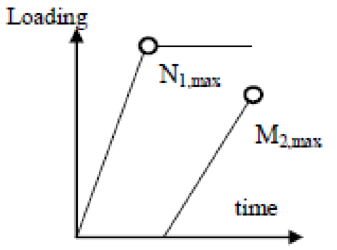 Initial axial load $N_{1,max}$ Bending moment $M_{2,max}$

8. Task 4 : cracked elbows

It is proposed in this section to compare the different procedures for the analytical J calculation for elbows with a surface crack

- the first list concerns pure mechanical loadings for elbows with a circumferential defect
- the second list concerns pure mechanical loadings for elbows with an axial defect
- the third list concerns pure thermal and combined mechanical & thermal loadings for elbows with a circumferential or an axial defect

For each case, the geometry and the material are specified. A loading variation is proposed. The extremes of this variation are specified. For the analyses, each phase of the mechanical loading variation will be decomposed into 5 steps. When the case concerns are combined mechanical & thermal loading condition, the initial values (elastic and elastic-plastic) for the initial mechanical loading have to be calculated.

Specific answer sheets are provided in appendix 2. It is asked to calculate the elastic and elastic-plastic value of J. If possible, the reference stress can be also introduced in the result tables.

8.1. Material properties

Two materials are considered for the following analyses.

8.1.1. material n6

E (MPa)	ν	$\sigma_{y,0.2\%}$ (MPa)	ALFA (°C^{-1})	n	σ_0 (MPa)	α
174700	0.3	185.1	1.81E-05	6	163	1.00E+00

SIG (MPa)	EPS (%)	SIG (MPa)	EPS (%)
0	0.000E+00	210	5.469E-01
10	5.724E-03	220	6.900E-01
20	1.145E-02	230	8.681E-01
30	1.718E-02	240	1.088E+00
40	2.292E-02	250	1.358E+00
50	2.870E-02	260	1.686E+00
60	3.458E-02	270	2.082E+00
70	4.065E-02	280	2.558E+00
80	4.710E-02	290	3.125E+00
90	5.416E-02	300	3.798E+00
100	6.222E-02	310	4.593E+00
110	7.178E-02	320	5.525E+00
120	8.354E-02	330	6.614E+00
130	9.843E-02	340	7.880E+00
140	1.176E-01	350	9.345E+00
150	1.425E-01	360	1.103E+01
160	1.750E-01	370	1.298E+01
170	2.174E-01	380	1.520E+01
180	2.722E-01	390	1.773E+01
190	3.428E-01	400	2.061E+01
200	4.329E-01	500	4.938E+01

8. Task 4 : cracked elbows

It is proposed in this section to compare the different procedures for the analytical J calculation for elbows with a surface crack

- the first list concerns pure mechanical loadings for elbows with a circumferential defect
- the second list concerns pure mechanical loadings for elbows with an axial defect
- the third list concerns pure thermal and combined mechanical & thermal loadings for elbows with a circumferential or an axial defect

For each case, the geometry and the material are specified. A loading variation is proposed. The extremes of this variation are specified. For the analyses, each phase of the mechanical loading variation will be decomposed into 5 steps. When the case concerns are combined mechanical & thermal loading condition, the initial values (elastic and elastic-plastic) for the initial mechanical loading have to be calculated.

Specific answer sheets are provided in appendix 2. It is asked to calculate the elastic and elastic-plastic value of J. If possible, the reference stress can be also introduced in the result tables.

8.1. Material properties

Two materials are considered for the following analyses.

8.1.1. material n6

E (MPa)	ν	$\sigma_{y,0.2\%}$ (MPa)	ALFA (°C^{-1})	n	σ_0 (MPa)	α
174700	0.3	185.1	1.81E-05	6	163	1.00E+00

SIG (MPa)	EPS (%)	SIG (MPa)	EPS (%)
0	0.000E+00	210	5.469E-01
10	5.724E-03	220	6.900E-01
20	1.145E-02	230	8.681E-01
30	1.718E-02	240	1.088E+00
40	2.292E-02	250	1.358E+00
50	2.870E-02	260	1.686E+00
60	3.458E-02	270	2.082E+00
70	4.065E-02	280	2.558E+00
80	4.710E-02	290	3.125E+00
90	5.416E-02	300	3.798E+00
100	6.222E-02	310	4.593E+00
110	7.178E-02	320	5.525E+00
120	8.354E-02	330	6.614E+00
130	9.843E-02	340	7.880E+00
140	1.176E-01	350	9.345E+00
150	1.425E-01	360	1.103E+01
160	1.750E-01	370	1.298E+01
170	2.174E-01	380	1.520E+01
180	2.722E-01	390	1.773E+01
190	3.428E-01	400	2.061E+01
200	4.329E-01	500	4.938E+01

AEN NEA IAGE Integrity of Components and Structures OECD

Case #	Geometry		Material	Loading	
Elbow C2	CDAI a (mm) h (mm) De (mm) Rc (mm) ψ_c (°) θ (°)	- 10 40 840 1600 90 -90	n6	P_{max} = 30 MPa	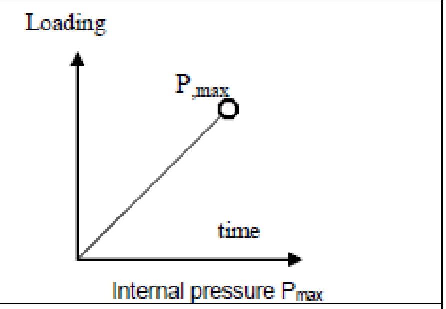
Elbow C3	CDAI a (mm) h (mm) De (mm) Rc (mm) ψ_c (°) θ (°)	- 10 40 840 1600 90 -90	n6	$M_{2,max}$ = -6E9 N.mm	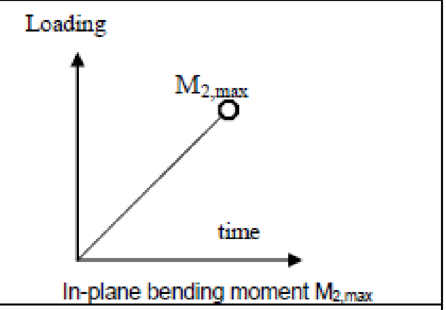
Elbow C6	CDSI a (mm) h (mm) De (mm) Rc (mm) ψ_c (°) θ (°) c (mm)	- 10 40 840 2400 90 90 30	n6ter	P_{max} = 28 MPa	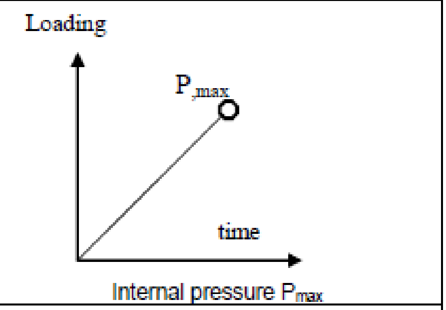
Elbow C7	CDSI a (mm) h (mm) De (mm) Rc (mm) ψ_c (°) θ (°) c (mm)	- 10 40 840 1600 90 90 30	n6ter	$M_{2,max}$ = -6E9 N.mm	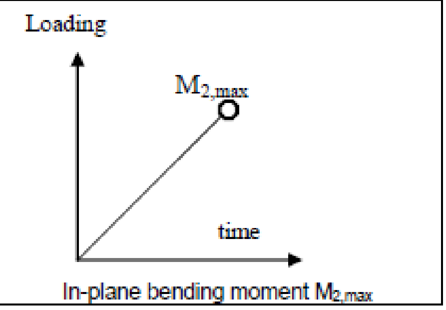

Case #	Geometry		Material	Loading	
Elbow C9	CDSI a (mm) h (mm) De (mm) Rc (mm) ψ_c (°) θ (°) c (mm)	- 10 40 840 1600 90 171 30	n6	$M_{3,max}$ = 4,92E9 N.mm	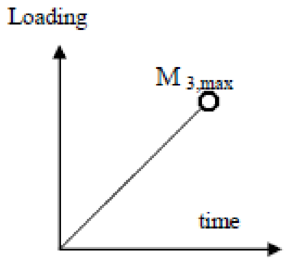 Out-of-plane bending moment $M_{3,max}$
Elbow C13	CDAI a (mm) h (mm) De (mm) Rc (mm) ψ_c (°) θ (°)	- 10 40 840 1600 90 -90	n6	P_{max} = 20 MPa $M_{2,max}$ = -4E9 N.mm	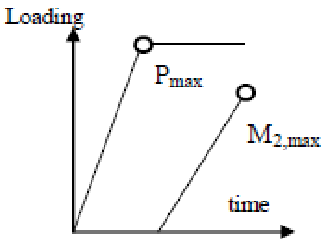 Initial pressure P_{max} Bending moment $M_{2,max}$
Elbow C14	CDSI a (mm) h (mm) De (mm) Rc (mm) ψ_c (°) θ (°) c (mm)	- 10 40 840 2400 90 177 30	n6	$M_{1,max}$ = -4,6E9 N.mm $M_{3,max}$ = 4,6E9 N.mm	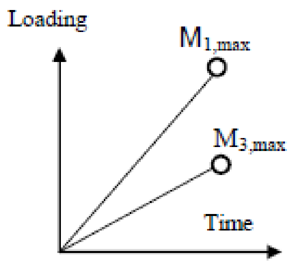 Torsion moment $M_{1,max}$ Out-of-plane bending moment $M_{3,max}$

8.3. axial cracks

Case #	Geometry		Material	Loading	
Elbow L1	LDII a (mm) h (mm) De (mm) Rc (mm) ψ_c (°) θ (°)	- 10 40 840 1600 90 -90	n6ter	P_{max} = 30 MPa	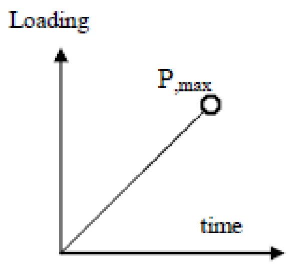 Internal pressure P_{max}
Elbow L3	LDII a (mm) h (mm) De (mm) Rc (mm) ψ_c (°) θ (°)	- 10 40 840 1600 90 -90	n6ter	$M_{2,max}$ = -4,5E9 N.mm	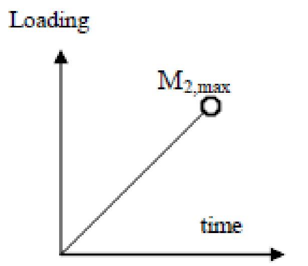 In-plane bending moment $M_{2,max}$
Elbow L6	LDSI a (mm) h (mm) De (mm) Rc (mm) ψ_c (°) θ (°) c (mm)	- 10 40 840 1600 90 90 30	n6ter	P_{max} = 30 MPa	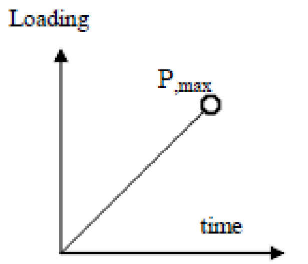 Internal pressure P_{max}
Elbow L13	LDSE a (mm) h (mm) De (mm) Rc (mm) ψ_c (°) θ (°) c (mm)	- 10 40 840 1600 90 -90 30	n6ter	$M_{2,max}$ = -5,8E9 N.mm	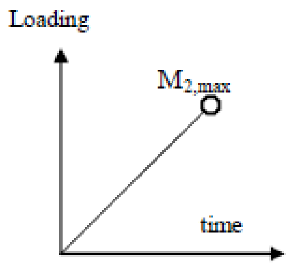 In-plane bending moment $M_{2,max}$

AEN NEA — IAGE Integrity of Components and Structures — OECD

Case #	Geometry		Material	Loading	
Elbow L17	LDSI a (mm) h (mm) De (mm) Rc (mm) ψ_c (°) θ (°) c (mm)	- 10 40 840 1600 45 -90 30	n6ter	P_{max} = 10 MPa $M_{2,max}$ = -5E9 N.mm	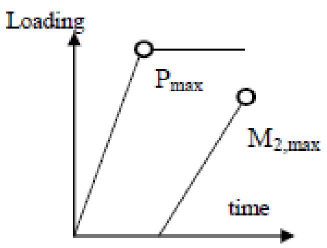 Initial pressure P_{max} In-plane bending moment $M_{2,max}$
Elbow L20	LDSI a (mm) h (mm) De (mm) Rc (mm) ψ_c (°) θ (°) c (mm)	- 10 40 840 1600 90 -90 30	n6ter	$M_{2,max}$ = 5E9 N.mm $M_{3,max}$ = 5E9 N.mm	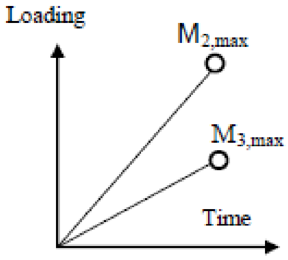 In-plane bending moment $M_{2,max}$ Out-of-plane bending moment $M_{3,max}$

8.4. Elementary thermal and combined Mechanical & thermal loads

Case #	Geometry		Material	Loading	
Elbow L23	LDSI a (mm) h (mm) De (mm) Rc (mm) ψ_c (°) θ (°) c (mm)	- 10 40 840 1600 90 90 30	n6ter	$\Delta T_{1,max}$ = 357.4 °C $\Delta T_{2,max} / \Delta T_{1,max}$ = 0.178	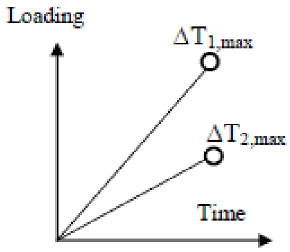 Trough thickness temperature linear variation $\Delta T_{1,max}$ $\Delta T_{2,max} / \Delta T_{1,max}$ = constant
Elbow L27	LDSI a (mm) h (mm) De (mm) Rc (mm) ψ_c (°) θ (°) c (mm)	- 10 40 840 1600 90 -90 30	n6ter	$\Delta T_{1,max}$ = 357.4 °C $\Delta T_{2,max} / \Delta T_{1,max}$ = 0.178 $M_{2,max}$ = -2.05e9 N.mm	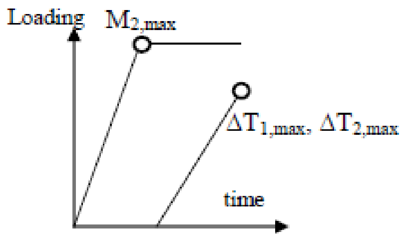 Trough thickness temperature linear variation $\Delta T_{1,max}$ $\Delta T_{2,max} / \Delta T_{1,max}$ = constant Initial bending moment $M_{2,max}$

Case #	Geometry		Material	Loading	
Elbow C30	CDSI a (mm) h (mm) De (mm) Rc (mm) ψ_c (°) θ (°) c (mm)	- 10 40 840 1600 90 90 30	n6ter	$\Delta T_{1,max}$ = 357.4 °C $\Delta T_{2,max} / \Delta T_{1,max}$ = 0.178 $M_{2,max}$ = -2.05e9 N.mm	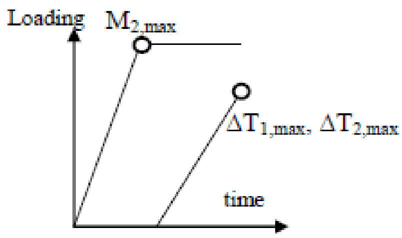 Trough thickness temperature linear variation $\Delta T_{1,max}$ $\Delta T_{2,max} / \Delta T_{1,max}$ = constant Initial bending moment $M_{2,max}$

9. Task 5 : particular cases

This chapter propose more specific situation. For each case, an answer sheet is available in the appendix 3.

9.1. Imposed displacement loading condition

This first particular case concerns a cracked pipe submitted to an imposed axial displacement.

The external radius of the pipe is 60 mm, the thickness 10 mm and the pipe length 64.5 mm. The defect is a circumferential axisymetric defect with a = 2.5 mm.

One section is embedded. The opposite section is submitted to an uniform axial displacement u_z=0.645 mm.

The material properties are given in the following tables :

$Rp_{0,2}$ (MPa)	R_m (MPa)	Elongation (%)	Kv
322	485	30.3	144

ε (%)	σ (MPa)
0	0
0.18	344.0
2.6	409.5
3	427.7
3.5	455
4	464.1
4.5	482.3
5	500.5
6	527.8
7	546
8	564.2
9	582.4

ε (%)	σ (MPa)
10	600.6
11	614.2
16	659.7
20	691.6
25	747.9
30	798.9
35	849.9
40	900.9
50	1002.8
60	1104.8
100	1512.6

It is proposed to calculate into 5 steps the elastic and the elastic-plastic values of J.

Use the answer sheet proposed in the appendix 3.1.

9.2. embedded cracks

This second particular case proposes to calculate the elastic stress intensity factor for an internal defect :

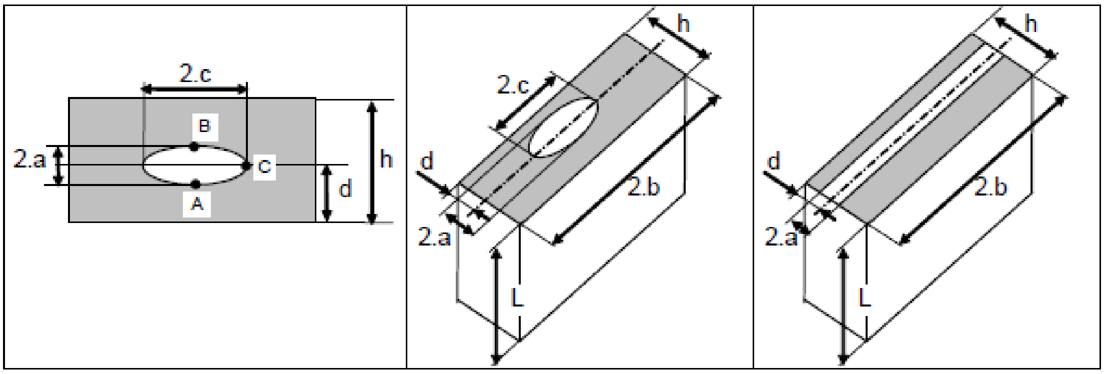

The plate geometry is h = 10 mm and 2b = 350 mm, and is submitted to :

-an axial loading N1 = 3.5 e6 N

- a bending moment M2 = 6E5 N.mm

It is asked to calculate the elastic stress intensity factor for following defects :

2a/h	0.1	0.5
d/h	0.1, 0.3, 0.5	0.3, 0.5
c/a	1, 3, 6, ∞	

Use the answer sheet proposed in the appendix 3.2.

9.3. underclad cracks

The case is a thermal shock imposed to a PWR vessel containing a trough-clad defect. The following tables provide all data needed for the analysis : geometry, thermal and mechanical properties, fluid temperature variation.

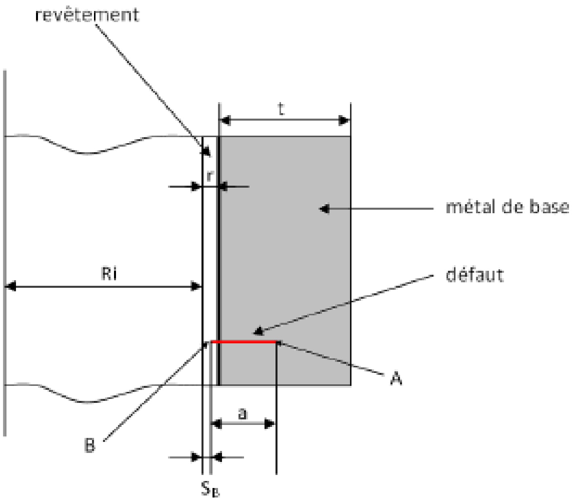

Ri	Internal radius [mm]	2500
r	Cladding thickness (mm)	7.5
t	Ferritic vessel thickness (mm)	200
S_B	Distance between the crack tip B and the internal surface (mm)	r (the crack is only in the ferritic metal)

	Ferritic vessel	cladding
Thermal conductivity λ [$W.m^{-1}.°C^{-1}$]	45.8	18.6
Specific heat C_p [$J.kg^{-1}.°C^{-1}$]	569	569
Young modulus g E [MPa]	199000	199000
Strain hardening modulus E_T [Mpa.mm/mm]	-	2000
Poisson coefficient ν	0.3	0.3
Yield stress σ_y [Mpa]	517	270
Thermal dilatation coefficient α between 20°C & T [10^{-6} °C^{-1}]	13.3	17

The thermal transient is given in the following table :

t (s)	P (MPa)	Tf (°C)	H (W/m².°C)
0	15.5	286	174000
50	11.8	283	174000
100	8	280	43600
300	7	266	21200
520	6.4	250	2700
600	5.5	227	3200
700	5	202	3200
740	4.8	192	3200
800	4.5	170	3200
1000	3.5	114	3000
1300	2	64	2500
1800	2	27	1900
2800	2	10	1400
3800	2	7	1200
4800	2	7	1000
6300.001	2	7	800

The defect is an under clad crack (see following figure).

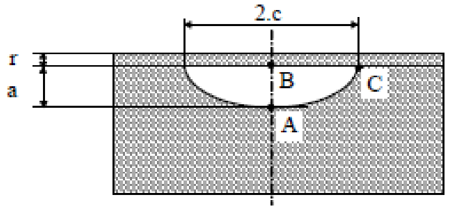

Under clad defect

It is asked to calculate the elastic stress intensity factor K_I and 'equivalent elastic-plastic' stress intensity factor $K_{I,cp}$ at the deepest point of the defect A, the point B and the surface point C for the semi-elliptical defect sizes given in the following table :

a (mm)	6	12
c/a	1, 3, 6, ∞	

Use the answer sheet proposed in the appendix 3.3.

9.4. through clad defects

The case is a thermal shock imposed to a PWR vessel containing a trough-clad defect. The following tables provide all data needed for the analysis : geometry, thermal and mechanical properties, fluid temperature variation.

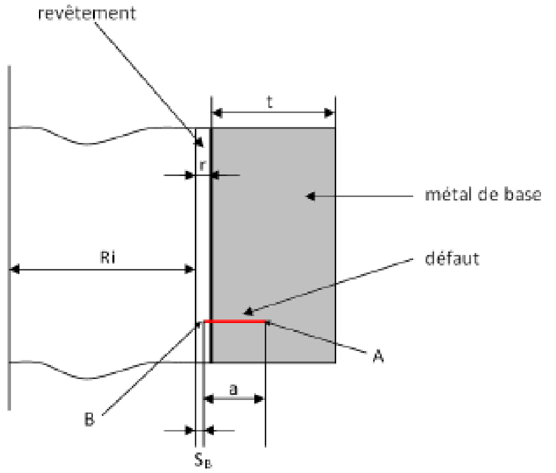

Ri	Internal radius [mm]	2500
r	Cladding thickness (mm)	7.5
t	Ferritic vessel thickness (mm)	200
S_B	Distance between the crack tip B and the internal surface (mm)	r (the crack is only in the ferritic metal)

	Ferritic vessel	cladding
Thermal conductivity λ [$W.m^{-1}.°C^{-1}$]	45.8	18.6
Specific heat C_p [$J.kg^{-1}.°C^{-1}$]	569	569
Young modulus g E [MPa]	199000	199000
Strain hardening modulus E_T [Mpa.mm/mm]	-	2000
Poisson coefficient ν	0.3	0.3
Yield stress σ_y [Mpa]	517	270
Thermal dilatation coefficient α between 20°C & T [10^{-6} °C^{-1}]	13.3	17

The thermal transient is given in the following table :

t (s)	P (MPa)	Tf (°C)	H (W/m².°C)
0	15.5	286	174000
50	11.8	283	174000
100	8	280	43600
300	7	266	21200
520	6.4	250	2700
600	5.5	227	3200
700	5	202	3200
740	4.8	192	3200
800	4.5	170	3200
1000	3.5	114	3000
1300	2	64	2500
1800	2	27	1900
2800	2	10	1400
3800	2	7	1200
4800	2	7	1000
6300.001	2	7	800

The defect is a through wall crack (see following figure).

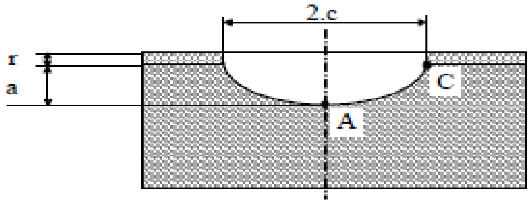

Through clad defect

It is asked to calculate the elastic stress intensity factor K_I and 'equivalent elastic-plastic' stress intensity factor $K_{I,cp}$ at the deepest point of the defect ands the surface point for the semi-elliptical defect sizes given in the following table :

-

a (mm)	6	12
c/a	1, 3, 6, ∞	

Use the answer sheet proposed in the appendix 3.3.

9.5. Stratification loading

in complement of your benchmarkcases proposition and as you suggest, I would like to propose and additional example dedicated to thermal loading, and in particular to a stratification loading.

The geometry in consideration is a pipe defined by De = 932 mm, h = 76 mm, half length =1033 mm

The defect is a large part-through wall semi-elliptical circumferential defect (CDSI) defined by : a/h = 0.75 andc/a = 4.

The material in question is an austenitic stainless steel with E = 176500 MPa, nu = 0.3 and Alpha = 1.71E-5

True stress-strain curve is the following :

Eps	Sig
0	0
0.000635	112
0.000749	114.5
0.00086	117
0.00118	120.4
0.00171	125.2
0.00274	131
0.00479	138.9
0.00682	145.2
0.00885	150.3
0.0109	155.3
0.0159	165.6
0.021	175.5
0.0311	193.2
0.0513	225.2
0.1017	299.7
0.152	357.5
0.303	446.6
0.503	531.7
1.004	668.8
5.006	1113.3

The loading is made of 2 composants :

- First, limited internal pressure : Pmax = 1 MPa
- Then global linear thermal gradient through the pipe section (global stratification) : DT = 0 to 300°C

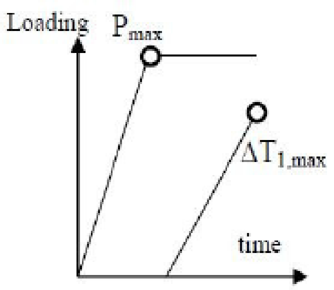

The pipe rotation is fixed at both end sections (but not translation) so that stratification creates global bendig stresses. Of course, the defect is located in the symetry plane of the loading with the deepest point at the maximum loading location.

AEN NEA IAGE Integrity of Components and Structures OECD

For that case, I will provide elastic and elastic-plastic reference F.E. solutions. Personnaly I will apply RSE-M and R6 formalisms, the objective being to evaluate how these approaches could evaluate accurately (at minimum conservatively) such thermal loading configuration.

10. Task 6: Consequences of welds

10.1. Materials

10.1.1. material AL10

E (MPa)	ν	$\sigma_{y,0.2\%}$ (MPa)	ALFA (°C^{-1})	n	σ_0 (MPa)	α
172000	0.3	132	-	-	-	-

SIG (MPa)	EPS (%)
0.000	0
128.342	0.07461715
132.000	0.27674419
1484.491	75

10.1.2. material AL15

E (MPa)	ν	$\sigma_{y,0.2\%}$ (MPa)	ALFA (°C^{-1})	n	σ_0 (MPa)	α
172000	0.3	198	-	-	-	-

SIG (MPa)	EPS (%)
0.000	0.000
192.483	0.112
198.000	0.315
2225.695	75.000

10.1.3. material AL23

E (MPa)	ν	$\sigma_{y,0.2\%}$ (MPa)	ALFA (°C^{-1})	n	σ_0 (MPa)	α
172000	0.3	304	-	-	-	-

SIG (MPa)	EPS (%)
0.000	0.000
302.049	0.176
304.000	0.377
1027.846	75.000

10.1.4. material RO10

E (MPa)	ν	$\sigma_{y,0.2\%}$ (MPa)	ALFA (°C^{-1})	n	σ_0 (MPa)	α
172000	0.3	132	-	-	-	-

SIG (MPa)	EPS (%)	SIG (MPa)	EPS (%)
0	0.000	191.4	2.111
2.5	0.001	204.8	3.119
17.1	0.010	214.9	4.125
53.9	0.032	223	5.130
68	0.044	229.9	6.134
79.2	0.056	235.9	7.137
95.1	0.085	241.2	8.140
106.7	0.122	246	9.143
116.2	0.168	250.3	10.146
124.3	0.222	258.1	12.150
130.4	0.276	264.8	14.154
139.5	0.381	270.7	16.157
146.4	0.485	276.1	18.161
156.6	0.691	281	20.163
164.3	0.896	291.7	25.170
170.6	1.099	300.6	30.175
182.5	1.606		

10.1.5. material RO15

E (MPa)	ν	$\sigma_{y,0.2\%}$ (MPa)	ALFA (°C^{-1})	n	σ_0 (MPa)	α
172000	0.3	132	-	-	-	-

SIG (MPa)	EPS (%)	SIG (MPa)	EPS (%)
0	0.000	190	0.214
17.2	0.010	200	0.328
50	0.029	210	0.542
60	0.035	220	0.933
70	0.041	230	1.630
80	0.047	240	2.860
90	0.052	250	4.970
100	0.058	260	8.500
110	0.064	270	14.300
120	0.070	280	23.700
130	0.076	290	38.700
140	0.083	300	62.100
150	0.091	310	98.100
160	0.102	320	153.000
170	0.121	330	235.000
180	0.153		

AEN NEA — IAGE Integrity of Components and Structures — OECD

10.1.6. material RO23

E (MPa)	ν	$\sigma_{y,0.2\%}$ (MPa)	ALFA (°C^{-1})	n	σ_0 (MPa)	α
172000	0.3	304	-	-	-	-

SIG (MPa)	EPS (%)	SIG (MPa)	EPS (%)
0	0.000	349.6	2.203
54.5	0.032	359.9	3.209
124	0.072	367.3	4.214
203.1	0.119	373.2	5.217
224.3	0.134	378.1	6.220
239.4	0.149	382.3	7.222
259	0.181	386	8.224
272.1	0.218	389.2	9.226
282.2	0.264	392.2	10.228
290.5	0.319	397.3	12.231
296.6	0.372	401.7	14.234
305.3	0.477	405.6	16.236
311.6	0.581	409	18.238
320.8	0.787	412.1	20.240
327.4	0.990	418.7	25.243
332.7	1.193	424.2	30.247
342.5	1.699		

10.2. Circumferential surface crack in the middle of a weld joint

All defects are located in the middle of the weld joint (position 1 in the following figure).

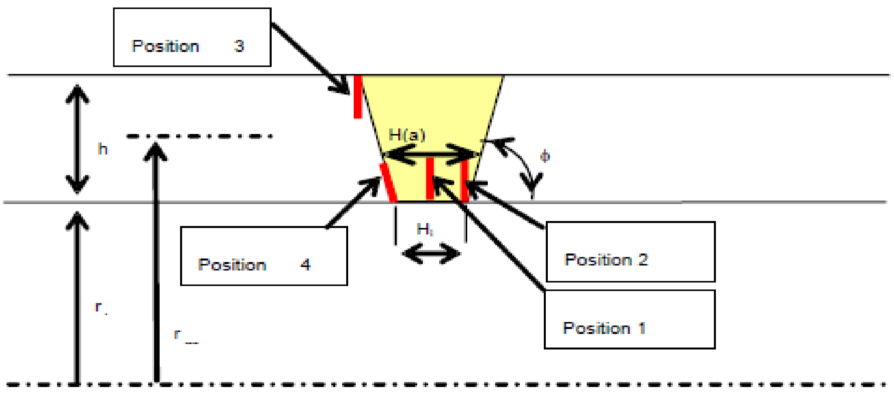

AEN NEA   IAGE Integrity of Components and Structures   OECD

Case #	Geometry		Material	Loading	
Pipe W2	CDAI D_e (mm) h (mm) a (mm) Hi (mm) ϕ (°)	- 660 60 15 10 90	Base metal : RO10 Weld : RO15	$N_{1,max}$ = 2E7 N	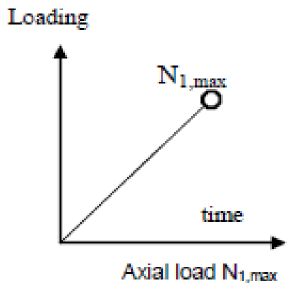
Pipe W5	CDAI D_e (mm) h (mm) a (mm) hi (mm) ϕ (°)	- 660 60 15 10 90	Base metal : RO10 Weld : RO23	$N_{1,max}$ = 2E7 N	
Pipe W6	CDAI D_e (mm) h (mm) a (mm) Hi (mm) ϕ (°)	- 660 60 3.75 10 90	Base metal : RO10 Weld : RO23	$N_{1,max}$ = 2,88E7 N	
Pipe W8	CDAI D_e (mm) h (mm) a (mm) Hi (mm) ϕ (°)	- 660 60 15 10 60	Base metal : RO10 Weld : RO23	P_{max} = 30 MPa $N_{1,max}$ = 1,68E7 N	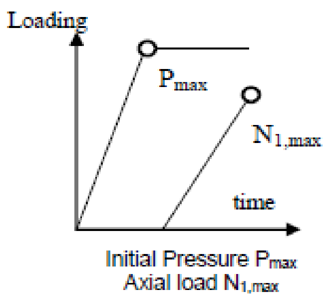
Pipe W9	CDAI D_e (mm) h (mm) a (mm) Hi (mm) ϕ (°)	- 660 60 15 10 60	Base metal : BL10 Weld : BL23	P_{max} = 30 MPa $N_{1,max}$ = 1,5E7 N	
Pipe W11	CDSI D_e (mm) h (mm) a (mm) c (mm) Hi (mm) ϕ (°)	- 660 60 3.75 3.75 10 60	Base metal : RO10 Weld : RO23	$M_{2,max}$ = 6,69E9 N.mm	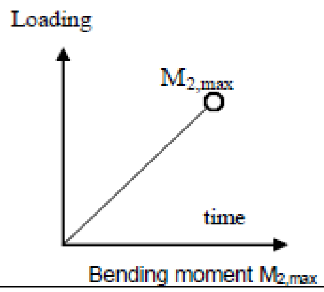
Pipe W13	CDSI D_e (mm) h (mm) a (mm) c (mm) Hi (mm) ϕ (°)	- 660 60 15 15 10 60	Base metal : RO10 Weld : RO23	P_{max} = 60 MPa	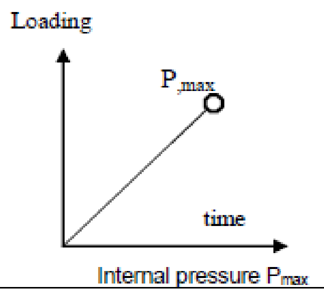

AEN NEA | IAGE Integrity of Components and Structures | OECD

Pipe W14	CDSI D_e (mm) h (mm) a (mm) c (mm) hi (mm) ϕ (°)	- 660 60 15 15 10 60	Base metal : RO10 Weld : RO23	$M_{2,max}$ = 6E9 N.mm	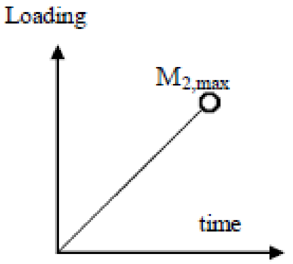 Bending moment $M_{2,max}$

AEN NEA IAGE Integrity of Components and Structures OECD

11. Organisation-planning

01/01/2011 Draft benchmark send for review to potential participant

01/03/2011 Participant send to CEA :

- The official contact name
- Comments and questions on the document
- List of items on which they will contribute
- Eventual additional cases

04/04/2011 CEA report to IAGE meeting : official start of the benchmark

01/07/2011 Deadline for submission of the results for task 1 – K evaluation

18/07/2011 Side meeting during 2011 PVP conference

01/12/2011 Deadline for submission of the results for task 2 & 3 – J evaluation for pipes with a surface and a through wall defect

**/04/2012 CEA report to IAGE meeting : progress of the benchmark

01/07/2012 Deadline for submission of the results for task 4 – J evaluation for elbows with a surface defect

18/07/2012 Side meeting during 2012 PVP conference

18/07/2012 Side meeting during PVP conference

01/12/2012 Deadline for submission of the results for task 5 – particular cases & task 6 – Influence of welds

01/03/2013 first draft of the benchmark final report

**/04/2013 CEA report to IAGE meeting : progress of the benchmark

**/07/2013 final meeting during 2013 PVP conference

01/12/2013 final report

**/04/2014 CEA report to IAGE meeting : conclusions of the benchmark

12. Task 7: Final report and recommendation

- Comparison of results for each task of the different procedures used by the benchmark participants
- Recommendation for the procedures improvements, future R&D and harmonization of the procedures

Appendix 1 : Answer sheet for task 1 – Elastic K evaluation

Appendix 1.1 - Answer form for K calculation in cracked pipe

Geometry #	PIPE K1
Loading condition #	

a/h	*c/a*	*KI_loading_condition 1*	*KI_loading_condition 2*
0.1			
0.25			
0.5			
0.75			

Use this table for PIPE K1, K2, K3, K4, K5

Appendix 1.2 - Answer form for K calculation in cracked plate

Geometry #	Plate

a/h	*KI*
0.1	
0.2	
0.3	
0.4	
0.5	
0.6	
0.7	
0.8	

AEN NEA IAGE Integrity of Components and Structures OECD

Appendix 2.3 – pure thermal loading

Geometry #	PIPE

Use this table for PIPE

Loading	DT1	DT2	KI	Elastic J	Elastic-plastic J
0.2DT1max					
0.4DT1max					
0.6DT1max					
0.8DT1max					
DT1max					

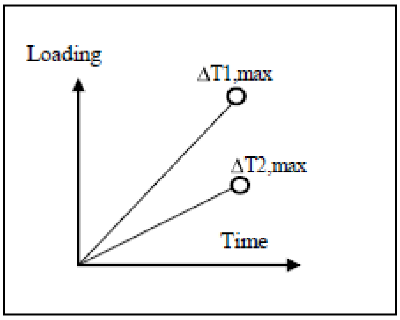

Appendix 2.4 – Combined Mechanical & thermal loading

Geometry #	PIPE

Use this table for PIPE

Mechanical loading (*)	Thermal loading	DT1	DT2	KItot	Elastic J	Elastic-plastic J
Lmax	0.DT1max					
Lmax	0.2DT1max					
Lmax	0.4DT1max					
Lmax	0.6DT1max					
Lmax	0.8DT1max					
Lmax	DT1max					

(*) Precise the nature of the Loading (P, M1, M2, M3)

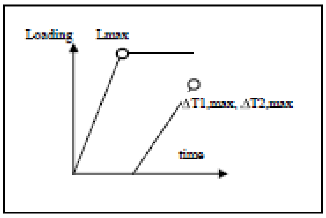

AEN NEA IAGE Integrity of Components and Structures OECD

Appendix 3 : Answer sheet for task 5 – particular cases

Appendix 3.1 – Pipe under axial displacement

Geometry #	Pipe under axial dispalcement

uz (mm)	Elastic J	Elastic-Plastic J
0.0645		
0.129		
0.1935		
0.258		
0.3225		
0.387		
0.4515		
0.516		
0.5805		

Appendix 3.2 – Plate with an emdebbed defect

Geometry #	Plate with an emdebbed defect

2a/h	d/h	c/a	KI
0.1	0.1	1	
		3	
		6	
		∞	
	0.3	1	
		3	
		6	
		∞	
	0.5	1	
		3	
		6	
		∞	
0.5	0.3	1	
		3	
		6	
		∞	
	0.5	1	
		3	
		6	
		∞	

<u>Appendix 3.3 – Cracked cladded vessel under thermal shock</u>

Geometry #	cracked cladded vesse lunder thermal shock
a	*
c	*

t	KI	KI,cp
0		
50		
100		
300		
520		
600		
700		
740		
800		
1000		
1300		
1800		
2800		
3800		
4800		
6300		

LIST OF PARTICIPANTS

	Name	**Company/Country**
1	S. Marie	CEA
2	S. Chapuliot	AREVA
3	H. Deschanels	AREVA
4	C. Faidy	EDF
5	P. Le Delliou	EDF
6	I. Hadley, S. Smith	TWI
7	P. Budden	BE
8	B. Brickstad	SSM
9	J. Gunnars	INSPECTA
10	S. Kamel	Imperial college
11	P. Frost	Fraze-Nash
12	Y.-J. Kim	Seoul University
13	K. Vaze	BARC
14	P. Chellapandi	IGCAR
15	Y.Takahashi	CRIEPI
16	D. Bernardi	ENEA
17	Z. Bin	NPIC
18	Y. Tang	RINPO
19	T. Palfi	VEIKI Hungary
20	T. Fekete	KFKI AEKI
21	S. Szavay	BAY-LOGI
22	L. Jurasek	IAM Brno
23	I. Simonovski	JRC Petten
24	K. Heckmann	GRS Germany
25	Angelo Maligno	United Kingdom
26	J. Sharples	United Kingdom